Electronic Thesis and Dissertation Repository

9-12-2017 2:30 PM

Elevated Temperature and CO2 Concentrations Affect Carbon Flux in Two Boreal Conifers

Sasha Madhavji, *The University of Western Ontario*

Supervisor: Danielle Way, *The University of Western Ontario*
A thesis submitted in partial fulfillment of the requirements for the Master of Science degree in Biology
© Sasha Madhavji 2017

Recommended Citation

Abstract

Elevated temperatures and CO_2 alter carbon flux in two dominant boreal tree species *Picea mariana* (black spruce) and *Larix laricina* (tamarack). Seedlings were grown in three temperature treatments (ambient, ambient +4 °C, and ambient +8 °C) at either 400 ppm or 750 ppm CO_2, to simulate climate conditions between now and the year 2100. Spruce acclimated to increasing temperature detractively; warming scenarios reduced spruce net carbon gain. Tamarack maintained comparable levels of net photosynthesis (A_{net}) across warming treatments and both species reduced respiration (R_{dark}) with increasing growth temperature. Elevated CO_2-grown spruce suppressed A_{net} whereas A_{net} in tamarack was unresponsive to elevated CO_2. Decreasing leaf N with warming explained reduced A_{net} and R_{dark} for both species; however, tamarack mitigated this by increasing stomatal conductance. Moderate warming benefited tamarack growth but hindered spruce; extreme warming hindered growth in both species. Reduced CO_2 uptake in these species with predicted warming may contribute to increased atmospheric CO_2 accumulation.

Keywords

Co-Authorship Statement

Experimental design was conceived with Dr. Danielle Way. I executed experiments, data analysis and interpretation, and the writing of this thesis. Editing was done by Drs. Danielle Way and Sheila Macfie. This project was part of a larger collaboration with Eric Dusenge.

Acknowledgments

I would like to thank my supervisor, Danielle Way for her guidance, support, and seemingly <u>infinite patience</u>; my advisory committee: Drs. Irena Creed and Sheila Macfie for aiding with experimental design and keeping me on track; colleagues in the Way lab for helping with training and data collection; and of course, Karen Nygard for her help with imaging. I would also like to thank Gord Thompson for his indispensable insight into O-rings; and lastly a special thanks to the Way lab volunteers: Cam, Nikki, Shaheer, and Sam—without whom this project would surely have never left the ground.

Table of Contents

List of Tables

List of Figures

List of Abbreviations

AC	Ambient CO_2 concentration
A_{net}	Net CO_2 assimilation rate
A_{opt}	Maximum A_{net}
ADP	Adenosine diphosphate
ATP	Adenosine triphosphate
C_a	Atmospheric CO_2 concentration
C_i	Intercellular CO_2 concentration
CO_2	Carbon dioxide
E	Transpiration rate
EC	Elevated CO_2 concentration (750 ppm)
$FADH_2$	Flavin adenine dinucleotide
FNR	Ferredoxin-NADP+ reductase
G3P	Glyceraldehyde 3-phosphate
g_s	Stomatal conductance
H	Hydrogen
LMA	Leaf mass per unit area
N	Nitrogen
NAD	Nicotinamide adenine dinucleotide
NADP	Nicotinamide adenine dinucleotide phosphate
O_2	Oxygen
P_i	Inorganic phosphate
PSI	Photosystem I
PSII	Photosystem II

R_{dark}	Dark respiration rate
R_{25}	R_{dark} measured at 25 °C
Rubisco	Ribulose-1, 5-bisphosphate carboxylase/oxygenase
RuBP	Ribulose-1, 5-bisphosphate
T0	Ambient temperature
T4	T0 + 4 °C (moderate warming)
T8	T0 + 8 °C (extreme warming)
T_m	Measurement temperature
T_{max}	High temperature CO_2 compensation point
T_{opt}	Thermal optimum of A_{net}
VPD	Vapour pressure deficit
WUE	Water use efficiency
2PG	2-phosphoglycolate

Chapter 1: Introduction

1.1 Climate change

The widespread combustion of fossil fuels and land use change since the Industrial

Revolution have caused atmospheric carbon dioxide (CO_2) concentrations to increase

from 280 ppm in 1880 to 400 ppm in 2016 (IPCC, 2014). Combustion of fossil fuels,

such as coal, natural gas and oil results in the production of CO_2, and autotrophic

photosynthesis is the primary process by which CO_2 is removed from the atmosphere.

While atmospheric CO_2 concentrations have only increased since the Industrial

Revolution, urban and agricultural expansion have resulted in widespread deforestation

around the world (Seto *et al*. 2012), reducing plant photosynthetic CO_2 uptake and long-

term CO_2 sequestration. The accumulation of CO_2 in the atmosphere traps radiation

emitted from the earth's surface below the atmosphere, driving the increase in global

surface temperature.

Since 1880, the global average surface temperature has increased by 0.65 °C and, if

current CO_2 emission trends continue, it is predicted to climb a further 4 °C by the end of

the 21st century (Ciais et al. 2014). By 2100, atmospheric CO_2 concentrations are

predicted to reach between 550 and 750 ppm, depending on the emissions scenario used

(IPCC, 2014). Even if worldwide greenhouse gas emissions ceased, global temperatures

would still rise by up to 1.7 °C by the end of the 21st century – a legacy of previously-

emitted CO_2 lingering in the atmosphere (IPCC, 2014). Warming is predicted to be

greater at high latitudes such that northern regions, such as the Arctic and boreal forest,

may warm up to 8 °C by 2100, partially due to a diminishing albedo effect as arctic sea ice melts and causes a positive feedback on regional temperature (Curry *et al.* 1995).

1.2 The boreal forest

The boreal forest is the largest terrestrial biome on the planet, and is characterized by long, harsh winters, short summers, strong seasonal climatic variability, and low precipitation. Tree species in the Canadian boreal forest are chiefly conifers, such as black spruce (*Picea mariana*), jack pine (*Pinus banksiana*), and tamarack (*Larix laricina*); some broadleaved species such as trembling aspen (*Populus tremuloides*) and paper birch (*Betula papyrifera*) also inhabit the forest (Tjoelker et al. 1998). Dominance of the forest stands by conifer trees leads to acidic soils, as decomposing needles release defensive compounds such as phenols, preventing many other plant types from growing on the forest floor (Rice and Pancholy 1974, Kuiters and Denneman 1987). The boreal forest faces regular, large-scale disturbances from forest fires and insect outbreaks (Kasischke et al. 1995, Bogdanski 2008), and is home to some of North America's most charismatic megafauna: wolves, caribou, grizzly bears, and lynxes. The extensive wetlands and peat bogs in the boreal forest are an integral part of both water cycling and filtration, as well as providing habitat to many species of waterfowl and other migratory birds (Bogdanski 2008).

In Canada, the boreal forest covers over half of the country's landmass and accounts for 77 % of the total forested area (Kurz and Apps 1999, Peng et al. 2011). 40 percent of the

nation's total wood production comes from the boreal forest, totalling an annual revenue of CA$41 billion and nearly 130,000 jobs (Bogdanski 2008). Beyond forestry, the boreal sector encompasses billions of dollars' worth of mining, agriculture, and hydroelectric energy, and sustains hundreds of thousands of jobs (Bogdanski 2008). The national-scale economics of the boreal forest are vast, but are perhaps eclipsed by the global significance of the forest in terms of atmospheric carbon dynamics. In Canada alone, the boreal forest stores 186 Gt of carbon in its living biomass, detritus, soils, and peat (Apps et al. 1993); it is estimated that 714 Gt of carbon are stored in the entire biome (Kasischke et al. 1995). Annually, the Canadian boreal drawdown of atmospheric CO_2 is approximately 95 Tg, making it a substantial carbon sink (Apps et al. 1993).

1.3 Black spruce and tamarack

Black spruce (*Picea mariana*) and tamarack (*Larix laricina*) are two dominant boreal conifer (cone-bearing) species; the former is evergreen, while the latter is a species of larch, and a deciduous conifer. Both species are gymnosperms from the Pinaceae (pine) family and are found throughout Canada and parts of Alaska – close relatives of these species inhabit the taiga of Eurasia (Gower and Richards 1990). Conifers have needle-shaped leaves and thrive in the harsh boreal environments where most broad-leaved tree species, excepting poplar and birch, cannot. High nutrient- and water-use efficiencies allow conifers to grow in boreal soils which are nutrient poor and often frozen or underlain by permafrost, limiting water uptake (Gower and Richards 1990, Givnish 2002). Nutrient limitation is partially caused by low rates of litter decomposition in cold temperatures (Kurz and Apps 1999, Robinson 2002). Both the evergreen and deciduous

leaf strategies allow for advantages and trade-offs which ultimately dictate species'

ability to survive and thrive in the harsh, cold climates of the boreal forest.

Evergreen needles have long lifespans and must withstand winter conditions which

deciduous leaves never experience. By investing in structural compounds, such as thick

cuticles, evergreen needles are able to endure wind shear, ice crystal abrasion, and snow

accumulation, but this comes at the expense of developing more metabolic machinery

(Givnish 2002, Van Ommen Kloeke et al. 2012). Evergreen needles typically have a low

nitrogen concentration, making them less appealing to herbivores (Mooney and Gulmon

1982). By investing in hardy, year-round needles, evergreens are able to gain carbon

steadily throughout winter, albeit at a slower rate than during the summer months (Van

Ommen Kloeke et al. 2012). Photosynthesis ceases in evergreens when the ground

freezes in winter and water lost from transpiration cannot be replenished (Troeng and

Linder 1982). Water supplies the electrons to chlorophyll in the light-dependent reactions

of photosynthesis (see Section 1.4.1) and frozen soil precludes water uptake by the roots,

temporarily halting the electron transport chain until water becomes available once more.

In contrast to black spruce, photosynthetic carbon gain in tamarack is constrained by the

limited growing season when needles are present. As such, tamarack need not invest as

heavily in structural tissue as an evergreen species, and instead generates "cheaper"

leaves which are able to photosynthesize at considerably higher rates than its sympatric

evergreen counterparts (Gower and Richards 1990, Givnish 2002, Van Ommen Kloeke et

al. 2012). By allocating less carbon to the structure of its needles, tamarack is able to build more leaves, allowing for fast growth rates; increased CO_2 diffusion through the comparatively thin needles of tamarack facilitates higher rates of photosynthesis, aided by high nitrogen investment per unit of leaf area. The deciduous strategy is consistent with opportunistic development during a shortened growing season: rapid, plastic response to environmental triggers, high rates of photosynthesis, and low leaf mass per unit area (Van Ommen Kloeke et al. 2012). By comparison, the evergreen strategy is conservative, both in metabolic rates and in response to environmental stimuli. Annual foliage regeneration is a costly process both energetically and in nutrient requirement, so evergreens are the predominant tree type of the boreal forest.

While the highly seasonal boreal conditions may be thought to favour an evergreen strategy, tamarack aboveground net primary productivity (NPP; gross carbon uptake minus respiratory carbon losses) exceeds that of deciduous broadleaf species and is commensurate with evergreen conifers (Gower and Richards 1990, Wright et al. 2004). Larch species inhabit boreal forests around the world and are able to optimize growth during a short growing season, allowing them to compete successfully with evergreen conifers. Allocation to root mass is lower in tamaracks than evergreen conifers, allowing them to compete for light by growing upwards and developing a full foliage (Gower and Richards 1990). Tamaracks have similar nitrogen use efficiency to evergreen conifers, but foliar nitrogen concentrations are up to 50 % higher in the deciduous species (Small, 1972, Gower and Richards, 1990, MacDonald and Lieffers, 1990), indicating a sizeable investment in metabolic enzymes such as Ribulose-1,5-bisphospate

carboxylase/oxygenase (Rubisco), which would allow for increased photosynthetic capacity. Perhaps the most unique feature enabling tamarack to survive in the boreal forest is its high nitrogen recycling in senescing needles. Tamaracks can retract up to 25 % more nitrogen from their needles before abscission than other boreal species, such as black spruce and paper birch, mitigating the high cost of the high leaf N and deciduous strategy (Chapin and Kedrowski 1983, Gower and Richards 1990, Givnish 2002).

1.4 Plant physiology

1.4.1 Photosynthesis

Photosynthesis is the process by which plants and other autotrophs create their own food – inorganic carbon dioxide (CO_2) is drawn from the air and fixed into sugars. This process is the foundation upon which all successive trophic layers are built; autotrophic carbon fixation is the only point in food webs where energy is stored in the bonds between carbon atoms in sugar molecules. Photosynthesis can be divided into two main parts: the light-dependent reactions of electron transport and the dark reactions of the Calvin-Benson cycle.

The light-dependent reactions begin in the thylakoid where light energy is harvested by pigment molecules such as chlorophyll. The pigment molecules absorb photons in the visible light spectrum; blue and red wavelengths are preferentially absorbed and yellow and green wavelengths are reflected, hence plants appear green in colour. The proteins of the light-dependent reactions are associated with the thylakoid membrane and begin with

Photosystem II (PSII) (Figure 1.1). As light strikes a leaf, pigment molecules, such as

chlorophyll, in PSII harvest energy from photons and transfer it to a pair of electrons

from a photo-dissociated water molecule. The electron transporter, plastoquinone, accepts

the excited electrons from PSII as well as a pair of H^+ ions from the chloroplast stroma,

both of which are transferred to the next major protein of the electron transport chain,

cytochrome b_6f. Cytochrome b_6f utilizes the energy from the excited electrons to pump

the H^+ ions across the thylakoid membrane into the thylakoid lumen, creating a high H^+

concentration relative to the chloroplast stroma. The electrons in cytochrome b_6f are

retuned to a low energy state after providing the energy to pump the H^+ ions, and are

transferred to Photosystem I (PSI) via the transporter plastocyanin where the electrons are

re-energized in the same manner as in PSII. The re-energized electrons are then passed on

from PS I to ferredoxin, and lastly to ferredoxin NADP+ oxioreductase (FNR). The last

protein in electron transport, FNR transfers the excited electrons to nicotinamide adenine

dinucleotide phosphate ($NADP^+$) to create NADPH in the chloroplast stroma.
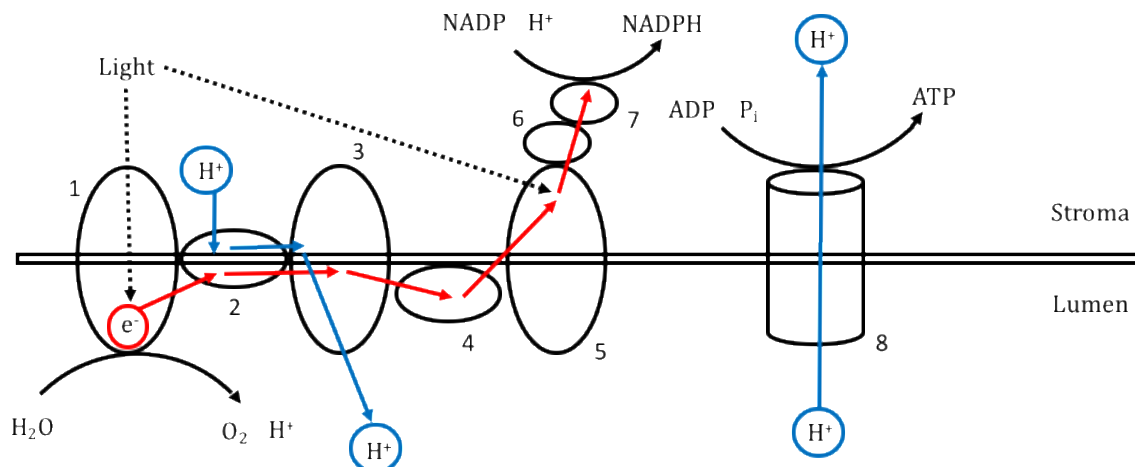
Figure 1.1 Schematic diagram of the enzymes involved in photosynthetic electron transport.

Electrons from a photo-dissociated water molecule are passed along a series of chloroplast membrane-associated enzymes: Photosystem II (1), plastoquinone (2), cytochrome b_6f (3), plastocyanin (4), Photosystem I (5), ferredoxin (6), and ferredoxin NADP+ oxioreductase (7). ATP synthase (8) generates adenosine triphosphate using a proton motive force. Red arrows represent the path of the excited electrons from a photo-dissociated water molecule and blue lines represent the points at which hydrogen ions cross the thylakoid membrane during photosynthetic electron transport. Black, dotted lines represent the path of light as it strikes the two Photosystems and solid, black, horizontal lines represent the thylakoid membrane.

NADPH is one of two major products of the light-dependent reactions and is used as a

reductant in the subsequent dark reactions (the Calvin Cycle). The final protein in the

electron transport chain (though itself not involved in the movement of electrons) is ATP

synthase. The high H^+ gradient in the thylakoid lumen is used to power the motor of ATP

synthase, which binds a molecule of inorganic phosphate (P_i) to adenosine diphosphate to

form adenosine triphosphate (ATP) in the chloroplast stroma. ATP is the other main

product of the light-dependent reaction and is used to fuel the Calvin Cycle. As

mentioned earlier, the electrons provided to the electron transport chain come from a

photo-dissociated water molecule; after passing on the excited electrons, PS II becomes a

strong oxidizing agent and breaks a water molecule apart into a pair of electrons and free

oxygen gas (the latter being a by-product of photosynthesis).

ATP and NADPH produced in the light-dependent reactions are used in the Calvin cycle,

which occurs in the chloroplast stroma. CO_2 diffuses through stomata in the leaf surface,

through the intercellular airspace of the leaf, into the mesophyll cells where

photosynthesis occurs and into the chloroplast, where it is fixed by the enzyme Rubisco

to the five-carbon molecule, Ribulose-1,5-bisphosphate (RuBP). The remaining steps in

the Calvin-Benson cycle consist of a series of reduction reactions which consume ATP

and NADPH from the light reactions to produce glyceraldehyde 3-phosphate (G3P – a

three carbon molecule). G3P is used to make sugars, such as glucose, as well as lipids

and polysaccharides, all of which are usable sources of energy for plant metabolic

processes, and to regenerate RuBP. Three turns of the Calvin Cycle regenerate three

molecules of RuBP and produce one extra G3P that is used to make glucose, which itself is made of two G3P molecules.

While the enzyme Rubisco fixes CO_2 in photosynthesis, it is a dual function enzyme and the active site is able to fix O_2 in a process known as photorespiration, which emits CO_2 (Figure 1.2). In photorespiration, Rubisco fixes O_2 to RuBP to produce G3P (albeit in half the quantity as would normally be in a carboxylation reaction) as well as 2-phosphoglycolate (2PG). To convert 2PG into G3P costs a molecule of ATP and releases one molecule of CO_2; therefore, photorespiration is both counterproductive to positive carbon assimilation in plants, and consumes ATP. Rubisco's relative affinity to O_2 and CO_2 changes with temperature and will be elaborated on in section 1.5.1.1. While photorespiration reduces plant carbon gain, it has been shown to play a role in protecting plants from radiative stress (Wingler et al. 2000). Photosynthesis itself defines the process by which plants fix CO_2; however, from a methodological standpoint, net CO_2 assimilation (A_{net}) is the relevant process to measure. A_{net} accounts for gross photosynthesis minus losses of CO_2 from photorespiration and mitochondrial respiration in the dark (R_{dark}) or light (R_{light}).
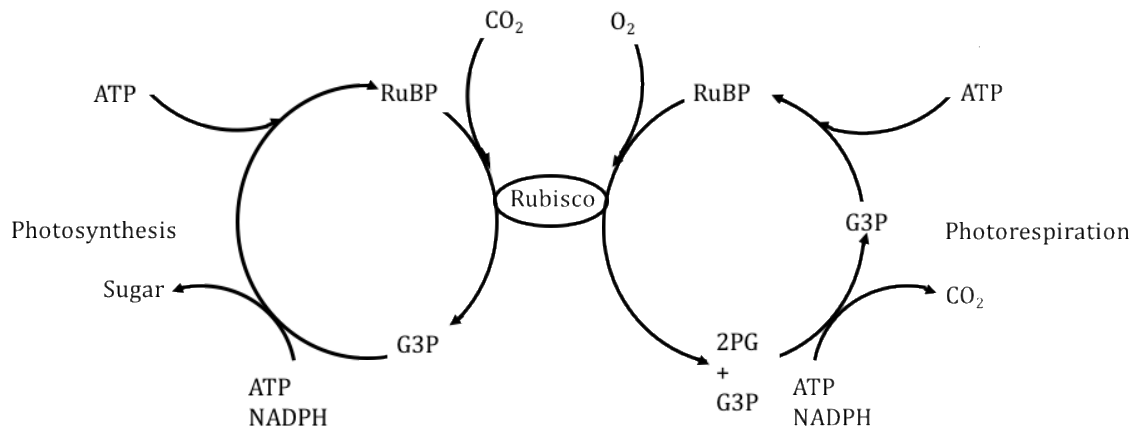
Figure 1.2 The dual pathways of the enzyme Ribulose-1, 5-Bisphosphate Carboxylase/Oxygenase (Rubisco).

Rubisco fixes either CO_2 (photosynthesis) or O_2 (photorespiration). The process of photosynthesis involves fixing incoming CO_2 to ribulose-1, 5-bisphosphate (RuBP) resulting in the generation of glyceraldehyde 3-phosphate (G3P), and the production of glucose. In photorespiration, O_2 is fixed to RuBP to produce 2-phosphoglycolate (2PG); regenerating RuBP from 2PG does not result in sugar production, but emits CO_2 while still requiring the input of ATP and NADPH.

1.4.2 Respiration

The sugars produced in photosynthesis are the source of energy for the catabolic reactions of R_{dark}. The disaccharide sucrose is the primary form of energy transported throughout the plant via the phloem to be later broken down in sink tissues. Whereas photosynthesis occurs in the chloroplasts, and mainly in leaves, respiration takes place in the mitochondria in all living plant tissue. Respiration occurs in four steps: glycolysis, pyruvate oxidation, the Krebs cycle (also called the citric acid cycle), and the electron transport chain. The stepwise combustion of a single glucose molecule through redox reactions results in the net production of at least 30 ATP molecules by the end of the respiratory process.

Glycolysis occurs in the cytoplasm and involves the halving of a glucose molecule into two three-carbon molecules of pyruvate; two NAD^+ molecules are reduced to NADH in glycolysis and the electron acceptors and pyruvate are shuttled into the mitochondria. The ATP investment required to phosphorylate glucose can become a limiting factor in sustaining high rates of respiration (see section 1.5.2.2) (Atkin et al. 2000).

The processes of pyruvate oxidation and the Krebs cycle generate reducing agents in the forms of NADH and $FADH_2$, as well as two molecules of ATP per glucose molecule, and produce CO_2 as a waste product. Pyruvate is oxidized to form acetyl-coenzyme A, which is attached to a pre-existing four-carbon molecule, oxaloacetate, in the Krebs cycle. As

with the regeneration of RuBP in the Calvin-Benson cycle, oxaloacetate is continually regenerated in the Krebs cycle so that the cycle is perpetuated.

The reducing agents produced in the Krebs cycle then power the electron transport chain (ETC) by donating their electrons to a series of proteins embedded in the inner mitochondrial membrane. The sequence of ETC proteins is as follows: Complex I (NADH dehydrogenase), Complex II (succinate dehydrogenase), Complex III (cytochrome bc_1 complex), and Complex IV (cytochrome c oxidase) – the final electron acceptor of the sequence is oxygen (O_2), which, when reduced, forms H_2O. The energy derived from electron flow across the chain is used to pump protons into the intermembrane space and create an electrochemical gradient across the inner mitochondrial membrane. The protons then move down the proton gradient through ATP synthase, converting large amounts of ADP to ATP through oxidative phosphorylation. This step is ultimately how the energy stored in glucose is converted into usable energy (in the form of ATP) for the plant.

Measurements of A_{net} are derived from CO_2 taken up and O_2 emitted by the plant through photosynthesis, balanced with O_2 taken up and CO_2 emitted via respiration (and photorespiration, see above). In plants, respiration occurs both in the light and in darkness; however, from a methodological standpoint, it is difficult to measure A_{net} *and* isolate the CO_2 emitted from R_{light} from that emitted concurrently by photorespiration.

1.5 Climate change and plant metabolism

The increases in atmospheric CO_2 concentrations predicted for this century will have direct impacts on the ability of plants to take up CO_2 via photosynthesis. As well, because photosynthesis and respiration are both highly sensitive to temperature, it is crucial to examine how increases in global temperatures will influence plant carbon fluxes. Plant carbon balance is dictated by the amount of carbon taken in through photosynthesis minus carbon losses through respiration, photorespiration, root exudates, and emissions of volatile organic compounds. Climate-mediated changes in rates of photosynthesis and respiration will have substantial consequences for both individual leaf-level carbon balance and the overall productivity of plant populations and entire ecosystems. Ecosystem productivity is the rate at which biomass is created in an ecosystem, and the foundation of biomass creation is laid by inorganic carbon being made available through autotrophic photosynthesis. It is well understood that autotrophic carbon balance defines ecosystem productivity, and therefore energy flow through higher trophic levels; however, it is less clear how autotrophic carbon balance, which is affected by global climate, then feeds back to influence global climate.

High temperature-induced reduction in A_{net} by plants, either through decreased carbon uptake or by increased respiratory losses, can lead to a buildup of atmospheric CO_2, leading to a positive feedback effect on further warming (Ainsworth and Rogers 2007, Slot and Kitajima 2015). Possible increases in A_{net} resulting from enriched CO_2 in a

future world could offset warming-induced reductions in A_{net} and reduce atmospheric CO_2 concentrations (Ainsworth and Long 2017). Earth system models, used to predict climate trajectories for the coming century, require an in-depth understanding of how carbon fluxes in different species and plant functional types vary in response to climate drivers (i.e. rising CO_2 and temperature) if these models are to make accurate forecasts.

1.5.1 Short-term plant responses to temperature

1.5.1.1 Photosynthesis

At low leaf temperatures, A_{net} is low; as leaf temperature increases, A_{net} increases until it reaches a thermal optimum (T_{opt}), then declines (Berry and Bjorkman, 1980) (Figure 1.3). The T_{opt} of A_{net} is highly variable among species and the nature of A_{net} response to acute changes in temperature can differ among species. How A_{net} responds to a short term (minutes to hours) increase in leaf temperature therefore depends on the degree of warming and how close the initial leaf temperature is to the plant's T_{opt} (Way and Yamori 2014, Yamori et al. 2014). A cold-limited plant—one operating at a temperature below its T_{opt}—will exhibit an increase in A_{net} when exposed to warming. Conversely, if acute warming exceeds a plant's T_{opt}, A_{net} will decrease.
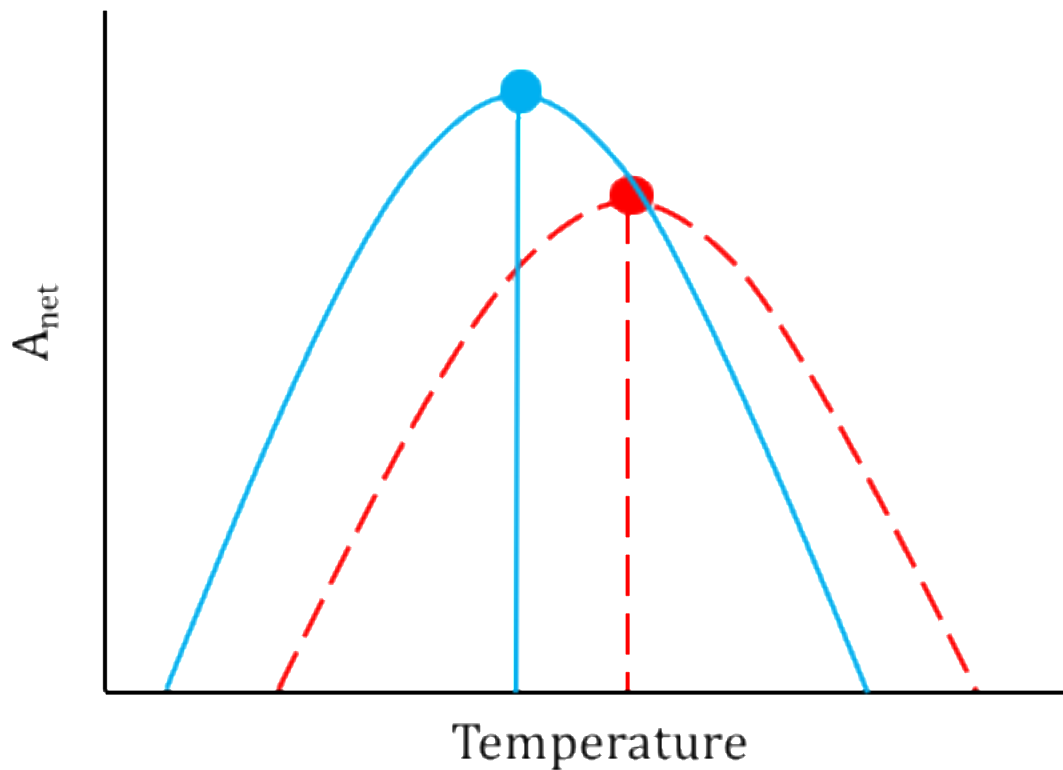
Figure 1.3 Thermal acclimation of net CO_2 assimilation rate (A_{net}) of a cold-grown plant and a warm-grown plant.

The warm-acclimated (dashed, red line) plant made constructive adjustments to the higher growth temperature by an increased thermal optimum of A_{net} (vertical line descending from apex) and a rightward shift in the entire A_{net} curve, indicating higher net CO_2 assimilation rates at higher temperatures that the cold-acclimated plant (solid, blue line). Detractive adjustment is seen in the warm-acclimated plant having a decreased A_{opt} (maximal rate of A_{net} at the T_{opt}; filled, red circle) compared to the cold-acclimated plant A_{opt} (filled, blue circle). Adapted from Way and Yamori (2014).

The T_{opt} of A_{net} is determined by the balance between respiration and photorespiration relative to photosynthesis; as temperatures increase past the T_{opt}, respiratory and photorespiratory losses eclipse carbon gain through photosynthesis. At extremely high temperatures, the thermal optimum of photosynthesis is determined by the heat stability of the photosynthetic apparatus and integrity of plant cell membranes (Hüve et al. 2011).Warming increases the fluidity of the plasma membrane and increases proton leakiness across the thylakoid membrane, reducing the efficiency of NADPH and ATP production in the light-dependent reactions of photosynthesis (Hazel 1995, Sage and Kubien 2007). Additionally, at temperatures above the thermal optimum of electron transport, cyclic electron flow can be induced as a method of photoprotection, diminishing NADPH production (Sharkey and Schrader, 2006). Moderate warming (up to 45 °C) does not have direct detrimental effects on the light harvesting complexes (Tang et al. 2006), however, increasing leaf temperature can have detrimental effects on the ability of Rubisco to carboxylate RuBP. The enzyme kinetics of Rubisco are highly temperature-sensitive; while carboxylation rates increase exponentially with increasing temperature and Rubisco is stable at temperatures of up to 50 °C (Crafts-Brandner and Salvucci 2000), Rubisco's chaperone enzyme, Rubisco activase, is heat-labile (Salvucci and Crafts-Brandner 2004, Sage et al. 2007, Holaday 2009). Rubisco activase maintains the activity of the active sites of Rubisco, but at high temperatures Rubisco activase cannot clear the catalytic sites of Rubisco fast enough to maintain Rubisco's carboxylation activity (Crafts-Brandner and Salvucci 2000). Rubisco is highly conserved among plant species, but the thermal properties of Rubisco activase are species-specific (Holaday

2009); beyond the optimal temperature for Rubisco activase function, denaturation of

Rubisco activase can reduce the carboxylation capacity of the plant.

In addition to the temperature sensitivity of Rubisco, Rubisco substrate specificity also

varies with temperature. Rubisco can fix either CO_2 or O_2 (photorespiration) but the

relative affinity of Rubisco for O_2 over CO_2 increases with increasing temperature

(Jordan and Ogren 1984). As well, the relative solubility of O_2 in air increases more

rapidly than does the solubility of CO_2 (Ku and Edwards 1977, Jordan and Ogren 1984).

The combined increase in photorespiration and decreased CO_2 solubility at high

temperatures serve to exacerbate thermal stress in plants at supra-optimal temperatures.

Vapour pressure deficit (VPD) is the difference between the amount of moisture held in

the air relative to the amount of moisture that could theoretically be held by saturated air.

Vapour pressure deficit will increase with temperature if there is not an increase in

relative humidity of the ambient air, resulting in an increase in leaf transpiration. Water

loss through increased transpiration can cause a plant to become water-stressed; to

combat water loss, plants will reduce their stomatal conductance, which, in turn, reduces

CO_2 uptake and thereby photosynthetic carbon gain (Way et al. 2015).

1.5.1.2 Respiration

As demonstrated above, fluctuations in temperature and CO_2 influence plant carbon gain; however, approximately half of a plant's carbon balance is dictated by carbon loss through respiration. Some plants can lose up to 80 % of their daily carbon gain through R_{dark}; on average across plant species, half of the carbon gained through photosynthesis is respired (Amthor 1991, Atkin and Tjoelker 2003). In accounting for plant carbon economics in a future world, it is then imperative to understand how R_{dark} responds to projected temperatures and CO_2 levels.

Typically, a linear increase in temperature results in an exponential increase in R_{dark} (Atkin and Tjoelker 2003). Unlike the parabolic response of photosynthesis to temperature, R_{dark} rates continue to increase at an exponential rate until the respiratory thermal optimum is reached. Increases in R_{dark} with high temperatures are caused by increased kinetic rates of mitochondrial enzymes (Raison et al. 1971). Beyond the thermal optimum, R_{dark} plummets as metabolic machinery succumbs to catastrophic heat stress: membranes are permanently damaged and enzymes denature (Hüve et al. 2011, Gauthier et al. 2014, O'Sullivan et al. 2016). It has been proposed that disintegration of mitochondrial membranes uncouple the processes of respiratory CO_2 release from electron transport at the high temperatures above the respiratory thermal optimum (i.e. > 50 °C) (Hüve et al. 2011). R_{dark} thermal optima are above 50 °C, much higher than the typical 25 °C thermal optimum of A_{net}. At temperatures exceeding the T_{opt} of A_{net} (though not high enough to cause respiratory failure), A_{net} declines while carbon loss continues to escalate.

1.5.2 Long-term plant response to temperature

1.5.2.1 Photosynthesis

If a plant remains in a warmed environment for several days to weeks, thermal acclimation can occur resulting in higher overall rates of A_{net} at the new, higher temperature (Yamori et al. 2014). Photosynthetic thermal acclimation can be evidenced by a higher thermal optimum of photosynthesis, a higher rate of photosynthesis at that thermal optimum, and/or a higher temperature at which carbon uptake and respiratory losses are in equilibrium (T_{max} – where A_{net} equals zero) (Way and Yamori 2014). If the acclimation of these photosynthetic parameters increases carbon gain in a warmed plant under its new growth temperature, this is termed "constructive adjustment"; acclimation of these parameters that does not increase carbon gain is called "detractive adjustment" (*sensu* Way and Yamori 2014) (Figure 1.3).

One of the key mechanisms of photosynthetic thermal acclimation in some species is the production of a heat-stable isoform of Rubisco activase (Law et al. 2001, Scafaro et al. 2016). This allows for a continually high activation state of Rubisco and allows for a warm-acclimated plant to maintain higher rates of carboxylation than a cold-acclimated plant at high temperatures (Sage et al. 2007). Warm-acclimated plants may also express heat shock proteins and chaperone proteins to stabilize protein synthesis at supra-optimal temperatures and repair proteins damaged by high heat (Yamori et al. 2014). Heat shock and chaperone proteins can also confer stability to plant cell membranes (maintaining homeoviscosity) to reduce proton leakiness and therefore electron transport inefficiency (Yamori et al. 2014).

1.5.2.2 Respiration

Plants can acclimate R_{dark} to warm temperatures over a period of several weeks to months such that plants acclimated to warm temperatures have lower rates of R_{dark} than cold-acclimated counterparts when measured at a common temperature (typically assessed at 25 °C) (Atkin and Tjoelker 2003). Classically, respiratory acclimation can be characterized as either Type I or Type II (Figure 1.4). Type I acclimation appears as a reduction in the slope of the exponentially increasing curve of R_{dark} with temperature in the warm-grown plant compared to a control plant (Atkin and Tjoelker 2003). The reduced slope of the R_{dark} temperature curve indicates a decreased respiratory thermal sensitivity, often measured as a Q_{10}. Q_{10} is the change in any physiological rate over a 10 °C increase in temperature; a Q_{10} of 2 means that the rate doubles over the given increase in temperature and a Q_{10} of 1 means that the rate has not changed in response to temperature (homeostasis).

Both Type I and Type II acclimation of respiration reduce the Q_{10} of R_{dark} in the warm-grown plant compared to the control plant. Type I acclimation yields similar rates of R_{dark} at cold temperatures but lowers R_{dark} rates at mid to high (10-35 °C) leaf temperatures (Atkin and Tjoelker 2003), and is thought to be due to substrate and adenylate limitations of R_{dark} at higher leaf temperatures (Atkin and Tjoelker 2003, Lee 2005). Type I acclimation is typical in cold-acclimated plants which are then subject to a degree of
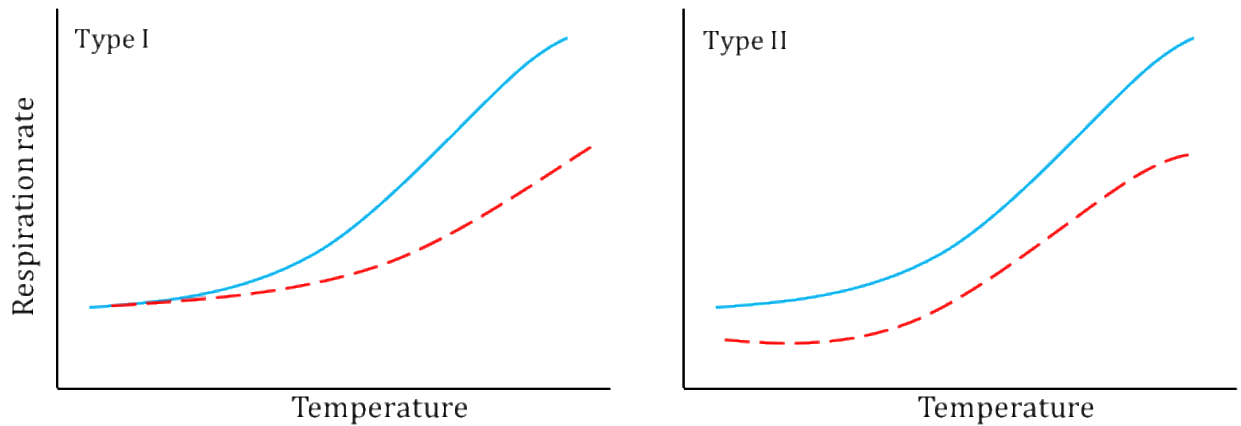
Figure 1.4 Two types of respiratory acclimation of a cold-grown and warm-grown plant.

Type I acclimation shows similar respiratory output of the two plants at low measurement temperatures, followed by a decreased slope in warm-acclimated respiration (dashed, red line) compared to a cold-acclimated plant (solid, blue line). There is no difference in the y-intercept of the respiration curves between a Type I-acclimated plant and a cold-acclimated plant. Type II acclimation shows a reduced rate of respiration across the entire range of measurement temperature for the warm-acclimated plant compared to the cold-acclimated plant. Type II acclimation is characterized by a decreased slope *and* y-intercept of respiration in a warm-grown plant. Adapted from Atkin and Tjoelker (2003).

warming over several weeks (Atkin and Tjoelker 2003). In contrast, Type II acclimation

of R_{dark} not only decreases the Q_{10} of R_{dark}, but also reduces the y-intercept of the R_{dark}

temperature response curve as well, such that rates of R_{dark} are reduced at all leaf

temperatures (Atkin and Tjoelker 2003). Type II acclimation results in a greater degree of

respiratory suppression than Type I acclimation and occurs via physical changes in the

respiratory machinery rather than solely by substrate and adenylate limitations (Atkin and

Tjoelker 2003, Campbell et al. 2007); Type II-acclimated plants may show decreases in

mitochondrial capacity and density, which may reduce the overall rate of respiratory

carbon loss (Klikoff 1966, Miroslavov and Kravkina 1991, Atkin and Tjoelker 2003).

Type II acclimation usually occurs in tissues which have developed in the new, warmer

environment and confers a greater degree of respiratory homeostasis than does Type I

acclimation (Atkin and Tjoelker 2003, Campbell et al. 2007).

1.5.3 Short-term plant response to CO_2

1.5.3.1 Photosynthesis

Exposure to high concentrations of CO_2 directly stimulates photosynthesis by increasing

the rate of Rubisco carboxylation and suppressing photorespiration (Ogren 1984). The

carboxylation rate increases due to increased CO_2 substrate availability, which also

effectively decreases photorespiration rates, since O_2 and CO_2 compete for the active site

of Rubisco. At low CO_2 concentrations (i.e., <150 ppm intercellular CO_2), photosynthesis

increases sharply as CO_2 concentrations increase, since the rate of Rubisco carboxylation

is the limiting step in net CO_2 assimilation (Sage and Kubien 2007). At high CO_2

concentrations (i.e. > 500 ppm), the supply of ATP and NADPH from photosynthetic

electron transport becomes limiting to photosynthesis, and further increases in CO_2 do not stimulate net CO_2 assimilation rates as much.

1.5.3.2 Respiration

Plant R_{dark} does not generally respond to changes in CO_2 concentration that occur over minutes to days. While it is methodologically complicated to measure R_{dark} over a range of ambient CO_2 concentrations using a standard portable photosynthesis system, studies using a variety of techniques (including isotopic techniques) have established that there is no instantaneous stimulation or suppression of R_{dark} by CO_2 (Amthor et al. 2001, Gonzalez-Meler et al. 2004).

1.5.4 Long-term plant response to CO_2

1.5.4.1 Photosynthesis

High CO_2-grown plants usually exhibit decreased A_{net} when compared to ambient CO_2-grown plants measured at a common CO_2 concentration – a consequence of photosynthetic down-regulation (Sage 1994). The primary mechanism behind long-term photosynthetic CO_2 acclimation is a buildup of excess carbohydrates in leaves under high CO_2 conditions (Moore et al. 1999, Lemoine et al. 2013). As carbon is fixed by Rubisco in the leaves, the resulting sugars are transported to source tissues via the phloem; CO_2-enriched plants produce sugars at a rate that eventually exceeds sink tissue demands (Lemoine et al. 2013). Increased sugars in leaf cells can supress the transcription of several Rubisco subunit proteins, thereby down-regulating photosynthesis (Moore et al.

1999). The enzyme hexokinase phosphorylates the six-carbon sugars produced from the Calvin-Benson cycle. As sugar concentrations rise within the cells of an elevated CO_2-grown plant, so too do hexokinase concentrations; elevated hexokinase levels act as a signal in the reduction of Rubisco subunit transcription (Moore et al. 1999).

The photosynthetic apparatus is costly in terms of plant nitrogen investment – Rubisco accounts for up to 30 % of a plant's nitrogen and 50 % of its soluble protein (Sage and Pearcy 1987, Feller et al. 2008). CO_2 acclimation reduces the amount of nitrogen devoted to photosynthetic enzymes, though this does not necessarily reduce A_{net} in an elevated CO_2-acclimated plant. The reduced nitrogen investment in photosynthetic enzymes resulting in lowered photosynthetic capacity is offset by a direct CO_2 enrichment effect in an elevated CO_2-acclimated plant *measured at its own growth CO_2 concentration* (Crous et al. 2008, 2013). Rates of A_{net} between ambient and elevated-CO_2 acclimated plants can be similar when measured in their respective growth CO_2 conditions – elevated CO_2 acclimated plants can even show higher rates of A_{net} in such cases (Ellsworth et al. 2004).

Additionally, stomatal conductance (g_s) decreases in plants acclimated to high CO_2, as less stomatal opening is required to maintain relatively high intracellular CO_2 concentrations (Way et al. 2015). Transpiration (E) then decreases as plants reduce their g_s over an acclimation period of several weeks, resulting in an increase in plant water use efficiency (WUE $= A_{net}/E$) (Ainsworth and Rogers 2007). High WUE can greatly benefit a plant as it mitigates water stress; however, decreased transpiration also reduces

evaporative cooling capabilities under high temperatures (Radin et al. 1994). Since high

temperatures will co-occur with increasing atmospheric CO_2 concentrations, reduced

evaporative cooling may exacerbate temperature stress for plants in a future world.

Additionally, reduced photosynthesis under CO_2-acclimated conditions, coupled with

reduced stomatal conductance, can significantly diminish plant carbon intake (Way et al.

2015).

1.5.4.2 Respiration

Acclimation of R_{dark} to elevated CO_2 is less straightforward than the acute response of

R_{dark} and results have varied across studies. Long-term growth in elevated CO_2 conditions

can lead to increased R_{dark} due to higher concentrations of foliar non-structural

carbohydrates (i.e. the respiratory substrate) (Gonzalez-Meler et al. 2004). Increased R_{dark}

can be further underpinned by increased mitochondrial density in leaves in plants that

develop at high CO_2 concentrations (Griffin et al. 2001, Armstrong *et al.* 2006a).

However, other studies have shown negligible, or even negative, effects of long-term

CO_2 exposure on R_{dark} rates; the lower nitrogen content of high CO_2-grown plants can

reduce respiratory capacity and could counteract any stimulation of R_{dark} via increased

respiratory substrate availability (Gonzalez-Meler et al. 2004).

1.6 Rationale and Objectives

The boreal forest represents a region of paramount importance, economically and

ecologically, not only for Canada, but the entire planet. As the world's largest terrestrial

biome, the boreal forest forms the foundation for significant biodiversity, as well as

crucial emergent properties of its innumerable ecosystems, such as water and nutrient

cycling. A significant proportion of the planet's CO_2 flows through the plants and soils of

the boreal forest, underscoring its pivotal role in a world increasingly imperiled by

greenhouse gas accumulation. As the climate in northern latitudes is expected to warm at

a higher rate than the rest of the world, it is important to understand how the projected

changes in climate will affect the species that dominate the CO_2 fluxes of the boreal

forest.

In my thesis, I investigated the physiological effects of elevated temperature and CO_2 on

two key boreal species: black spruce and tamarack. Specifically, I sought to elucidate the

capacity of these two species to acclimate CO_2 assimilation and respiration to increases in

temperature and CO_2 concentration. I hypothesized that, given that these species are

found in cold, harsh climates and are conservative compared to broad-leaved trees, they

will exhibit limited acclimation of A_{net} and R_{dark} to increasing temperature and CO_2.

Further, I hypothesized that tamarack, a deciduous species, will show a stronger

acclimation response than will black spruce, as the evergreen leaf strategy of the former

is consistent with limited, conservative response to environmental factors.

Future climate models require a high-resolution understanding of how species'

differential responses to climate drivers will feed back to influence the climate itself. The

work of my thesis will serve to increase the understanding of how two dominant boreal

species will respond to elevated temperature and CO_2, and how they will, in turn, affect CO_2 fluxes that feed back onto future climates.

Chapter 2: Materials and Methods

2.1 Experimental design

Seeds of *Larix laricina* (tamarack, from Finch Township, Ontario [45.133 °N, 75.083 °W]) and *Picea mariana* (black spruce, from Seed Zone 27, Ontario [46.522 °N, 80.953 °W]) were obtained from the National Seed Tree Centre in February, 2016 and stored at -20 °C until planted. The parent trees are from provenances that experience climatic conditions similar to London, Ontario, near the southern edge of the natural distribution of both species.

Seedlings were grown from seed in the Biotron Centre for Experimental Climate Change at the University of Western Ontario in London, Ontario, Canada (43.009 °N, 81.274 °W). One week prior to planting seeds, potting medium was prepared using Promix General-Purpose Mycorrhizae (Premier Tech, Rivière-du-Loup, QC) mixed with Miracle-Gro slow release fertilizer (The Scotts Miracle-Gro Company, Marysville, OH, USA), at a ratio of approximately 240 mL of fertilizer per 107 L of potting medium. The potting mix was then moistened and divided into 11.3 L pots, to create a total of 588 pots for the experiment.

Six temperature and CO_2 treatments were used for the study, with each treatment imposed in a separate climate-controlled greenhouse at the University of Western Ontario's Biotron Centre for Experimental Climate Change. The six treatments were: 1) ambient temperature (AT) with ambient CO_2 (400 $\mu mol\ mol^{-1}\ CO_2$; AC); 2) AT with

elevated CO_2 (750 μmol mol^{-1} CO_2; EC), 3) AT + 4 °C with AC, 4) AT + 4 °C with EC, 5) AT + 8 °C with AC, and 6) AT + 8 °C with EC. AT was determined by a five year (2006-2011) average of daily high and low temperature in London, Ontario and was ramped either up or down every 15 minutes between the two temperature points. Temperature control was maintained by an Argus Advanced Automated Control System (Argus Control Systems Ltd., Surrey, BC). The same system was also used to maintain CO_2 concentrations at 750 ppm in the EC greenhouses; AC air was pumped in from outdoors and then filtered. Relative humidity was maintained by the Argus system at a minimum of 60 %. The project took place in glass houses therefore photoperiod was that of daily London, Ontario for the duration of the growing season; however, shades were closed over the plants from 10:00 to 14:00 hours daily. The shades served to protect the seedlings from direct, brilliant sunlight.

On 1st May, 2016, 10 seeds of either tamarack or black spruce were planted into each of 49 pots per species per treatment, with a thin layer of perlite on top to prevent seeds from desiccating and being displaced when watered. Seeds were germinated in their respective growth treatments and pots were watered daily to field capacity. After two months of growth (July 2016), seedlings were thinned to one per pot, selecting for seedlings growing farthest from the edge of the pot. Throughout the growing period, plants were rotated periodically within their treatment to mitigate any potential effects of variation in watering and irradiance.

2.2 Gas exchange measurements

Four months after planting (September 1st, 2016), gas exchange measurements were

made on five random trees per species per treatment (n=5, N=60 seedlings for the

experiment). Gas exchange measurements were conducted using a Li-Cor 6400 XT (Li-

Cor BioSciences, Lincoln, NE, USA) which uses an infrared gas analyzer to measure

changes in CO2 and water concentration in order to calculate numerous plant

physiological parameters including rates of photosynthesis, respiration, and transpiration.

The Li-Cor forms an open flow system whereby air passes through a chamber containing

the leaf to be analyzed and concentrations of water vapour and CO_2 are compared

between ambient (reference) air before it goes through the cuvette and the air that is

passed through the chamber. There is one infrared gas analyzer measuring reference air

and another analyzer to measure the air after it passes over the plant sample; the

difference in water vapour and CO_2 concentrations are indicative of transpiration, and

photosynthetic and respiratory activity of the plant. Measurements were made in a walk-

in growth chamber (Environmental Growth Chambers, Chagrin Falls, OH, USA) to allow

the seedlings and gas exchange system to reach a full range of measurement

temperatures. Net CO_2 assimilation rates (A_{net}) and dark respiration rates (R_{dark}) were

measured at 10 °C, 15 °C, 20 °C, 25 °C, 30 °C, 35 °C, and 40 °C. At each temperature,

light-saturated A_{net} (measured at 1400 μmol photons m^{-2} s^{-1}) was first assessed at a

cuvette CO_2 concentration of 400 ppm, then at 750 ppm after A_{net} stabilized. The cuvette

CO_2 was then returned to 400 ppm, the cuvette irradiance was set to 0 μmol photons m^{-2}

s^{-1}, and R_{dark} was measured after a 20 minute dark-acclimation period. Only one

measurement CO_2 (400 ppm) was used in the R_{dark} measurements, as there is no direct

effect of measurement CO_2 on R_{dark} (Amthor et al. 2001). Vapour pressure deficit was maintained between approximately 0.5 and 4.5 kPa across the full 30 °C range of measurement temperatures for all gas exchange measurements. This measurement procedure was repeated at each of the seven measurement temperatures, resulting in two A_{net} temperature response curves (one at 400 ppm CO_2, the other at 750 ppm) and one R_{dark} temperature response curve for each tree.

After gas exchange was measured, needles from within the cuvette were stripped from the branch and photographed to analyze projected needle area (using Image J, US National Institutes of Health, Bestheda, MD, USA). The full gas exchange measurements of the 60 trees lasted from September 1st to October 31st 2016, and the treatments were repeatedly sampled in a rotating pattern to minimize any time effect on the variables.

2.3 Photosynthetic calculations

The photosynthetic thermal optimum (T_{opt}, the temperature at which the A_{net} is maximal) and the maximum A_{net} (A_{opt}, which occurs at T_{opt}) were derived from each individual A_{net} temperature response curve at each measurement CO_2 concentration by fitting a second-order polynomial to the data. This same equation was used to estimate T_{max}, the CO_2 compensation point (where A_{net} equals zero) above T_{opt}, which represents the maximum temperature at which photosynthetic carbon gain offsets respiratory carbon loss.

The calculations for gas exchange parameters were made according to the LI-COR 6400 manual. Values for A_{net} were estimated using equation (1)

$$A_{net} = \frac{F(C_r - C_s)}{100S} - C_s E \qquad (1)$$

where F denotes the air flow rate ($\mu mol\ s^{-1}$), C_r and C_s denote the reference and sample CO_2 concentrations, respectively, S denotes the leaf area (cm^2), and E denotes transpiration rate ($mol\ m^{-2}\ s^{-1}$). Transpiration (E) was calculated using equation (2)

$$E = \frac{F(W_s - W_r)}{100S(1000 - W_s)} \qquad (2)$$

where W_s and W_r denote the sample and reference water mole fractions (mmol H_2O (mol air)$^{-1}$), respectively. Lastly, stomatal conductance was calculated from equation (3)

$$g_{tw} = \frac{E\left(1000 - \frac{W_l + W_s}{2}\right)}{W_l - W_s} \qquad (3)$$

where g_{tw} denotes total conductance (stomatal conductance plus boundary layer condutance) and W_l denotes the water vapour concentration within the leaf (mmol H_2O (mol air)$^{-1}$).

2.4 Growth and nutrient analysis

Throughout the growing period of the experiment (May 1st to October 31st, 2016), trees were repeatedly measured for shoot height and stem diameter to formulate growth curves. Shoot height was measured using a ruler, starting at the soil line. Stem diameter was measured using a Vernier caliper at the point on the stem where it met the soil line.

Needles used in gas exchange measurements were dried at 60 °C until constant mass and

ground into powder using a Wiley mill (Thomas Scientific, Swedesboro, NJ, USA).

Approximately 5 mg of each powdered sample was analyzed for percent carbon and

nitrogen content using an elemental analyzer (Carlo Erba, Peypin, France). In elemental

analysis, samples are combusted instantaneously and the resulting gases emitted are

quantified by thermal conduction in a chromatographic column.

2.6 Statistical analysis

JMP software (SAS Institute, Cary, NC, USA) was used for all statistical analyses.

Temperature response curves of A_{net} at 400 ppm, A_{net} at 750 ppm and R_{dark} were assessed

with repeated-measures ANOVAs within each species, considering measurement

temperature, growth CO_2 and growth temperature. All other response variables were

assessed within each species using two-way ANOVAs for growth CO_2 and growth

temperature; a Tukey's Honest Significant Difference post-hoc test was used when

significant treatment effects were found.

Chapter 3: Results

3.1 Photosynthetic responses to growth temperature and CO_2

Moderate warming (T4) treatments were an average of 3.63 ± 0.090 °C warmer than ambient temperature (T0) treatments (Fig. 3.1A). Extreme warming (T8) treatments were an average of 3.81 ± 0.067 °C warmer than T4 treatments. Ambient CO_2 biomes maintained average CO_2 concentrations of 405.47 ± 1.96, 401.53 ± 2.75, and 414.32 ± 3.29 ppm CO_2 in the ACT8, ACT4, and ACT0 treatments, respectively (Figure 3.1B). Elevated CO_2 biomes maintained average CO_2 concentrations of 748.19 ± 0.31, 760.18 ± 1.58, and 743.02 ± 0.93 ppm CO_2 in the ECT8, ECT4, and ECT0 treatments, respectively.

3.1.1 Black spruce

3.1.1.1 Net CO_2 assimilation rate measured at a common CO_2 concentration of 400 ppm (A_{400})

There was no significant effect of growth temperature on A_{400} in spruce ($p = 0.12$); however, there was a trend for a growth CO_2 effect, as EC seedlings tended to have lower A_{400} than AC seedlings ($p = 0.086$; Figure 3.2A and B, Table 1). There was a significant effect of measurement temperature on A_{400} ($p < 0.0001$; Table 1); A_{400} was initially stimulated as leaf temperature increased above 10 °C, then declined beyond the T_{opt}. A significant interaction between growth temperature and growth CO_2 was found ($p = 0.014$), as EC seedlings had lower rates of A_{400} than AC seedlings in all temperature treatments. There was also a significant interaction of measurement temperature and
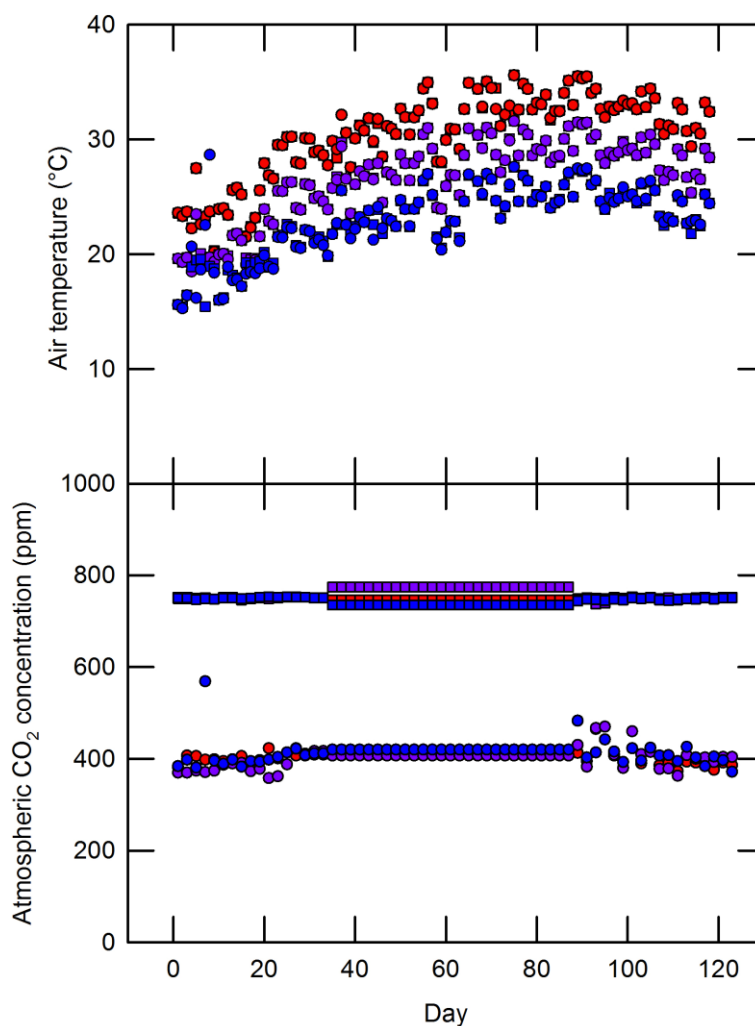
Figure 3.1 Temperature and CO_2 levels within the six biomes over the duration of the tree-growing period prior to all physiological experiments.

Day 0 indicates the day of seed planting (1st May, 2016) and all temperature (A) and CO_2 (B) readings shown were taken daily at noon, over the growing period. Blue symbols represent ambient temperature growth conditions (T0), purple symbols represent +4 °C-warmed growth conditions (T4), and red symbols represent +8 °C-warmed growth conditions. (8T) Circles represent ambient CO_2 growth conditions of 400 ppm, squares represent elevated CO_2 growth conditions of 750 ppm CO_2.
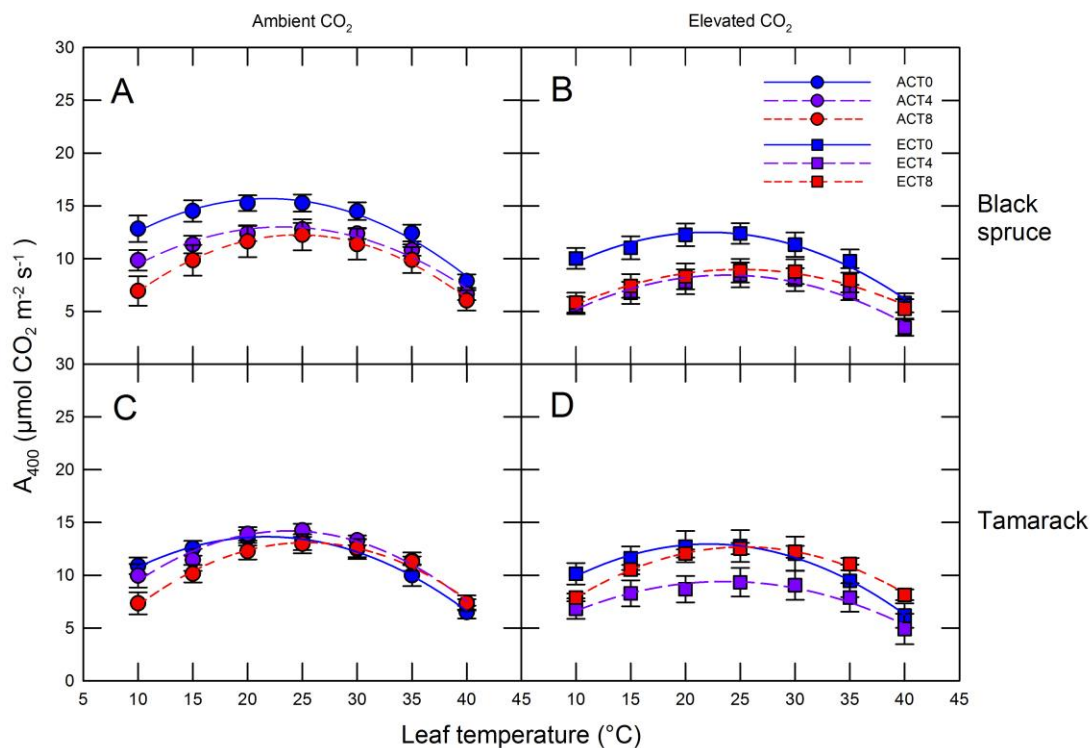
Figure 3.2 Net CO_2 assimilation rates of black spruce and tamarack measured at 400 ppm CO_2 (A_{400}).

Measurements were taken between leaf temperatures of 10 °C and 40 °C and at a saturating light level of 1400 µmol photons m^{-2} s^{-1}. Data shown as means ± SE, n = 5. Blue symbols and solid lines represent ambient temperature seedlings (T0), purple symbols and long-dashed lines represent +4 °C-warmed seedlings (T4), and red symbols and short-dashed lines represent +8 °C-warmed seedlings (8T). Circles represent ambient CO_2 growth conditions of 400 ppm (AC), squares represent elevated CO_2 growth conditions of 750 ppm CO_2 (EC).

growth CO_2 (p = 0.0024) in spruce as the temperature response of A_{400} in EC trees was shifted to the right of the response curve of AC trees. A significant interaction was found between measurement temperature and growth temperature (p = 0.0037), as T0 seedlings tended to have lower A_{400} at cool leaf temperatures and higher A_{400} at high leaf temperatures than T4 and T8 seedlings. Lastly, there was a significant interaction between measurement temperature, growth CO_2, and growth temperature (p = 0.0003; Table 1).

3.1.1.2 Net CO_2 assimilation rate measured at a common CO_2 concentration of 750 ppm (A_{750})

There was no significant effect of growth temperature (p = 0.21) on spruce A_{750} when measured at 750 ppm CO_2; however, there was a trend for a growth CO_2 effect (p = 0.093) as EC seedlings tended to have lower A_{750} than AC spruce (Figure 3.3A and B, Table 1). There was a significant effect of measurement temperature on A_{750} (p < 0.0001; Table 1); A_{750} was initially stimulated as leaf temperature increased above 10 °C, then declined beyond the T_{opt}. A significant interaction between growth temperature and growth CO_2 was found (p = 0.029) as ECT4 seedlings showed the lowest A_{750} of all three EC temperature treatments whereas ACT4 seedlings had middling A_{750} among the three temperature treatments. There was also a significant interaction between measurement temperature and growth CO_2 (p = 0.0063) in spruce. A significant interaction was found between measurement temperature and growth temperature (p = 0.032) whereby AT seedlings tended to assimilate CO_2 at higher rates than warmed seedlings across the

Table 1 Summary ANOVA statistics showing p-values for black spruce and tamarack gas exchange measurements of net CO_2 assimilation at 400 ppm measurement CO_2 (A_{400}), and 750 ppm measurement CO_2 (A_{750}).

Bolded p values are statistically significant ($p < 0.05$), italicized p values demonstrate $0.10 \geq p \geq 0.05$. T = growth temperature treatment, CO_2 = growth CO_2 concentration, and T_m = measurement leaf temperature.

	Black spruce	Tamarack	DF
A_{400}			
CO_2	*0.086*	0.59	1
T	0.12	0.70	2
T_m	**<0.0001**	**<0.0001**	6
$T \times CO_2$	**0.014**	0.14	2
$T_m \times CO_2$	**0.0024**	0.95	6
$T_m \times T$	**0.0037**	0.15	12
$T_m \times CO_2 \times T$	**0.0003**	0.64	12
A_{750}			
CO_2	*0.093*	0.9959	1
T	0.21	0.20	2
T_m	**<0.0001**	**<0.0001**	6
$T \times CO_2$	**0.029**	*0.082*	2
$T_m \times CO_2$	**0.0063**	0.88	6
$T_m \times T$	**0.032**	**0.011**	12
$T_m \times CO_2 \times T$	*0.052*	0.21	12
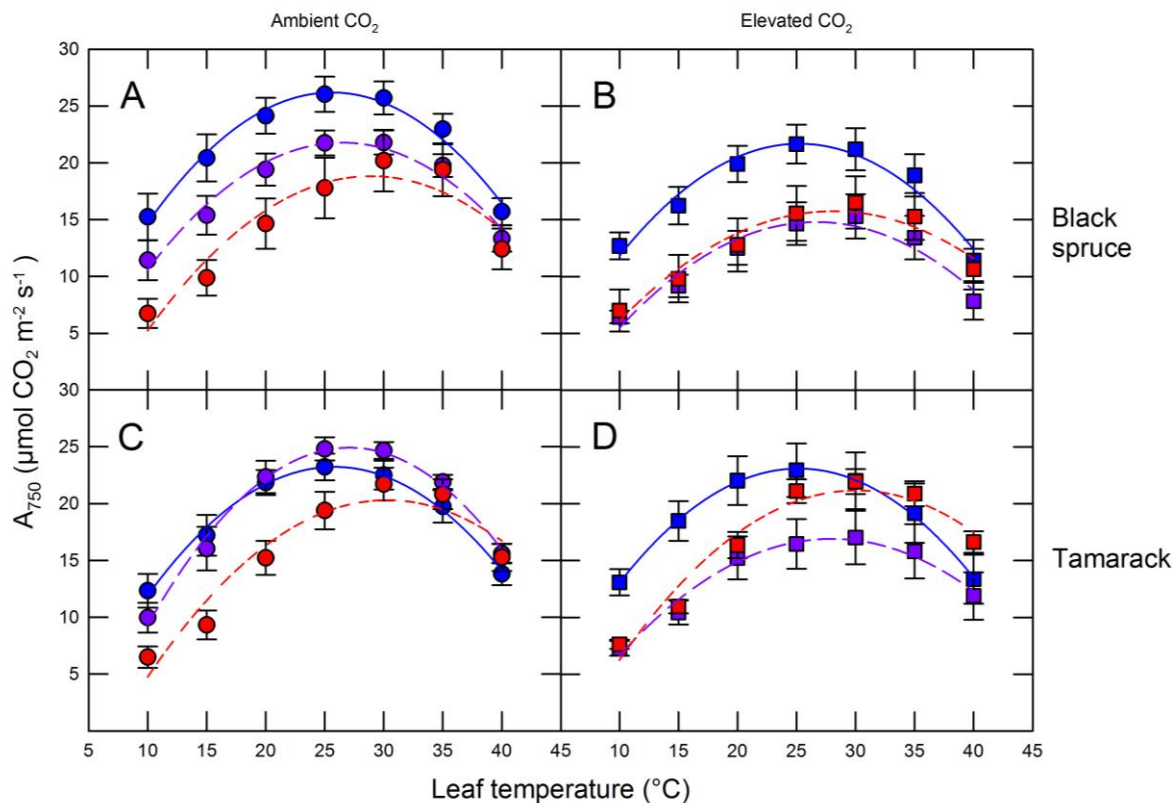
Figure 3.3 Net CO_2 assimilation rates of black spruce and tamarack measured at 750 ppm CO_2 (A_{750}).

Measurements were taken between leaf temperatures of 10 °C and 40 °C and a saturating light level of 1400 μmol photons m^{-2} s^{-1}. Data shown as means ± SE, n = 5. Blue symbols and solid lines represent ambient temperature seedlings (T0), purple symbols and long-dashed lines represent +4 °C-warmed seedlings (T4), and red symbols and short-dashed lines represent +8 °C-warmed seedlings (8T). Circles represent ambient CO_2 growth conditions of 400 ppm (AC), squares represent elevated CO_2 growth conditions of 750 ppm CO_2 (EC).

measurement temperature range. The interaction between measurement temperature, growth CO_2, and growth temperature was not significant but p = 0.052 (Table 1).

3.1.2 Tamarack

3.1.2.1 Net CO_2 assimilation rate measured at a common CO_2 concentration of 400 ppm (A_{400})

There was no significant effect of growth temperature (p = 0.70) on tamarack A_{400}, nor was there a growth CO_2 effect (p = 0.59; Figure 3.2C and D, Table 1). There was a significant effect of measurement temperature on A_{400} (p < 0.0001; Table 1); as in spruce, A_{400} was initially stimulated as leaf temperature increased above 10 °C, then declined beyond the T_{opt}. There was no significant interaction found between growth temperature and growth CO_2 (p = 0.14) nor between measurement temperature and growth CO_2 (p = 0.95) in tamarack. There was also no significant interaction between measurement temperature and growth temperature (p = 0.15). Lastly, there was no interaction between measurement temperature, growth CO_2, and growth temperature (p = 0.64; Table 1).

3.1.2.2 Net CO_2 assimilation rate measured at a common CO_2 concentration of 750 ppm (A_{750})

There was no significant effect of growth temperature (p = 0.20) or growth CO_2 (p=0.99) on tamarack A_{750} when measured at 750 ppm CO_2 (Figure 3.3C and D, Table 1). There was a significant effect of measurement temperature on A_{750} (p < 0.0001); A_{750} was initially stimulated as leaf temperature increased, then declined beyond the T_{opt}. There

was no interaction between growth temperature and growth CO_2 (p = 0.082) but ECT4

seedlings showed the lowest A_{750} of all three EC temperature treatments while ACT4

seedlings showed the highest A_{750} of all three AC temperature treatments. There was not,

however, a significant interaction of measurement temperature and growth CO_2 (p =

0.88) in tamarack. There was a significant interaction between measurement temperature

and growth temperature (p = 0.011), as the temperature response of A_{750} in T8 seedlings

was shifted towards higher leaf temperatures in comparison to T0 seedlings. Lastly, there

was no interaction found between measurement temperature, growth CO_2, and growth

temperature (p = 0.21; Table 1).

3.2 Stomatal conductance response to growth temperature and CO_2

3.2.1 Black spruce

There were no significant treatment effects of growth temperature (p = 0.31) or growth

CO_2 conditions (p = 0.35) on spruce stomatal conductance (g_s) when measured at 400

ppm CO_2 (g_{s400}), nor was there an interaction between the two (p = 0.97; Figure 3.4A and

B, Table 2). Measurement temperature did not have a significant effect on g_{s400} (p = 0.73)

nor was there an interaction between measurement temperature and growth CO_2 (p =

0.13; Table 2). There was a significant interaction between measurement temperature and

growth temperature (p = 0.010) as T0 seedlings consistently maintained the highest g_{s400}

across the measurement temperatures while warm-grown seedlings maintained lower

g_{s400}. Lastly, there was a significant interaction between measurement temperature,

growth temperature, and growth CO_2: EC trees had reduced g_{s400} in all temperature

treatments relative to AC trees, while ECT0 trees still maintained the highest g_{s400} compared to warm-grown EC trees (Figure 3.4A and B).

There were no significant treatment effects or interactions when spruce g_s was measured at 750 ppm CO_2 (g_{s750}; $p > 0.10$ for all; Figure 3.5A and B, Table 2) *except* for a significant interaction between measurement temperature, growth CO_2, and growth temperature ($p = 0.04$; Table 2); EC trees showed reduced g_{s750} compared to AC trees and ECT0 trees had the highest g_{s750} of all three EC temperature treatments (Figure 3.5A and B).

3.2.2 Tamarack

There were no significant treatment effects or interactions on tamarack g_{s400} ($p > 0.10$ for all; Figure 3.4C and D, Table 2). There were also no significant treatment effects or interactions on tamarack g_{s750} save for a trend of increasing g_{s750} with increasing measurement temperature ($p = 0.09$; Figure 3.5C and D, Table 2).
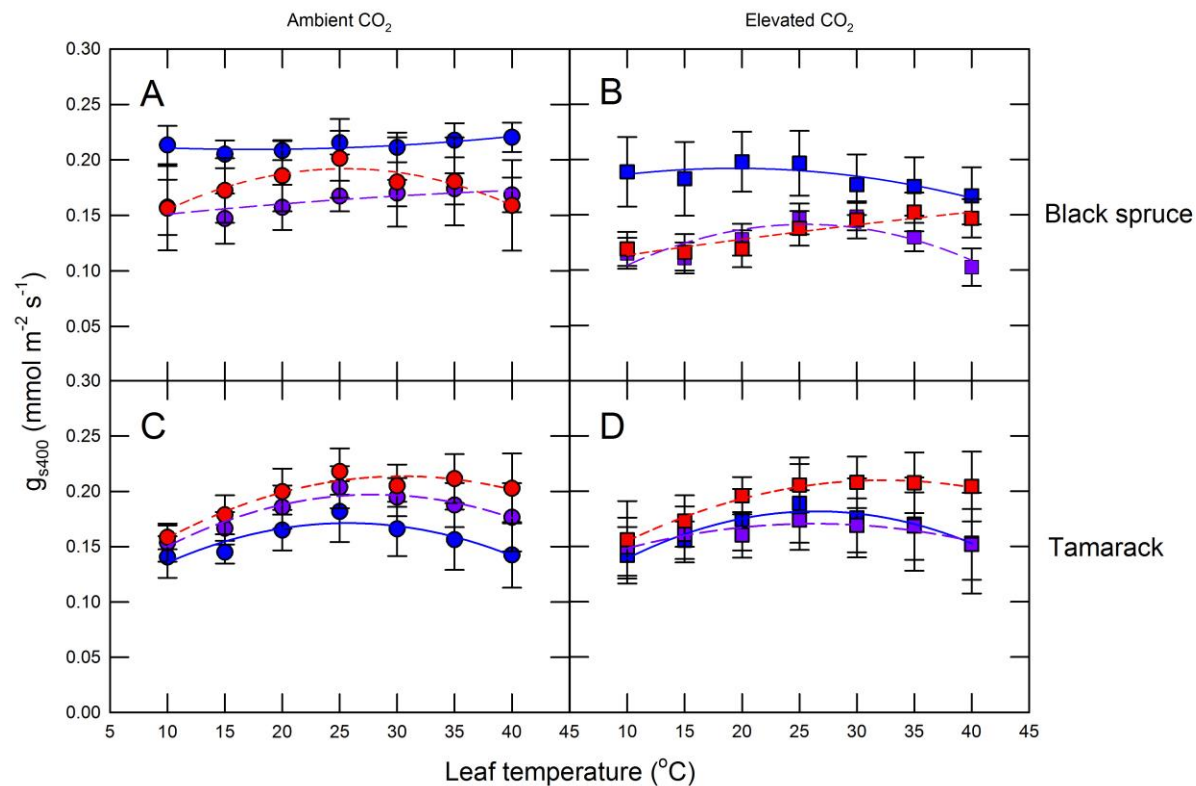
Figure 3.4 Stomatal conductance (g_{s400}) of black spruce and tamarack measured at 400 ppm CO_2.

Measurements were at a saturating light level of 1400 μmol photons m^{-2} s^{-1}. Data shown as means ± SE, n = 5. Blue symbols and solid lines represent ambient temperature seedlings (T0), purple symbols and long-dashed lines represent +4 °C-warmed seedlings (T4), and red symbols and short-dashed lines represent +8 °C-warmed seedlings. (8T) Circles represent ambient CO_2 growth conditions of 400 ppm (AC), squares represent elevated CO_2 growth conditions of 750 ppm CO_2 (EC).
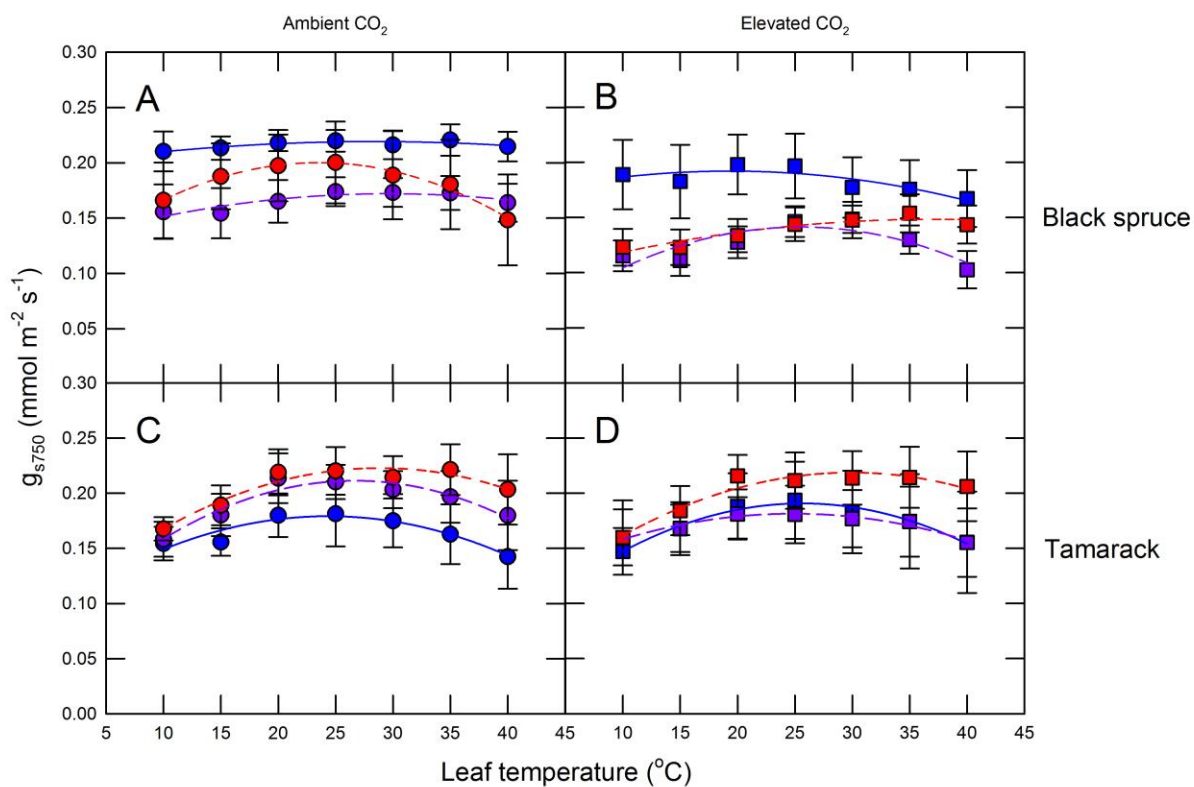
Figure 3.5 Stomatal conductance (g_{s750}) of black spruce and tamarack measured at 750 ppm CO_2.

Measurements were taken at a saturating light level of 1400 μmol photons m^{-2} s^{-1}. Data shown as means ± SE, n = 5. Blue symbols and solid lines represent ambient temperature seedlings (T0), purple symbols and long-dashed lines represent +4 °C-warmed seedlings (T4), and red symbols and short-dashed lines represent +8 °C-warmed seedlings (8T). Circles represent ambient CO_2 growth conditions of 400 ppm (AC), squares represent elevated CO_2 growth conditions of 750 ppm CO_2 (EC).

Table 2 Summary ANOVA statistics showing p-values for black spruce and tamarack stomatal conductance measured at a CO_2 concentration of 400 (g_{s400}) or 750 ppm (g_{s750}), and the ratio of intercellular to atmospheric CO_2 at a measurement CO_2 of 400 ppm (C_i/C_{a400}) and 750 ppm (C_i/C_{a750}). Bolded p values are statistically significant ($p < 0.05$), italicized p values represent $0.10 \geq p \geq 0.05$. T = growth temperature treatment, CO_2 = growth CO_2 concentration, and T_m = measurement leaf temperature.

	Black spruce	Tamarack	DF
g_{s400}			
CO_2	0.35	0.81	1
T	0.31	0.56	2
T_m	0.73	0.10	6
$T \times CO_2$	0.97	0.86	2
$T_m \times CO_2$	0.13	0.99	6
$T_m \times T$	**0.04**	0.98	12
$T_m \times CO_2 \times T$	**0.007**	0.99	12
g_{s750}			
CO_2	0.33	0.82	1
T	0.31	0.55	2
T_m	0.52	*0.09*	6
$T \times CO_2$	0.97	0.85	2
$T_m \times CO_2$	0.10	0.93	6
$T_m \times T$	0.16	0.96	12
$T_m \times CO_2 \times T$	**0.04**	0.96	12
C_i/C_{a400}			
CO_2	0.55	0.39	1
T	0.21	*0.09*	2
T_m	**<0.0001**	**<0.0001**	6
$T \times CO_2$	0.28	0.27	2
$T_m \times CO_2$	0.71	0.85	6
$T_m \times T$	0.52	0.20	12
$T_m \times CO_2 \times T$	0.45	0.69	12
C_i/C_{a750}			
CO_2	0.86	0.80	1
T	0.21	*0.07*	2
T_m	**<0.0001**	**<0.0001**	6
$T \times CO_2$	0.39	0.48	2
$T_m \times CO_2$	0.69	0.65	6
$T_m \times T$	*0.08*	0.24	12
$T_m \times CO_2 \times T$	0.25	0.98	12

3.3 C_i/C_a response to temperature and CO_2

3.3.1 Black spruce

There were no treatment effects or interactions on spruce intercellular CO_2 ratios when measured at 400 ppm CO_2 (C_i/C_{a400}; $p > 0.21$ for all; Figure 3.6A and B, Table 2); however, there was a strong measurement temperature effect ($p < 0.0001$) as C_i/C_{a400} decreased from 10 °C to 25 °C then increased again up to 40 °C (Figure 3.6A and B). When spruce intercellular CO_2 ratios were measured at 750 ppm CO_2 (C_i/C_{a750}), the same measurement temperature effect occurred ($p < 0.0001$) as well as a trend for higher C_i/C_{a750} in T8 trees compared to T4 and T0 trees ($p = 0.08$; Figure 3.7A and B, Table 2).

3.3.2 Tamarack

There was a trend for a growth temperature effect ($p = 0.090$) on tamarack C_i/C_{a400} as increasing growth temperature led to increased C_i/C_{a400}, but no significant growth treatment effects were found ($p > 0.20$ for all; Figure 3.6C and D, Table 2). There was, however, a similar effect of measurement temperature on tamarack C_i/C_{a400} ($p < 0.0001$) as was seen in spruce. Tamarack C_i/C_{a750} responded in much the same way as did C_i/C_{a400}: there was a growth temperature trend ($p = 0.070$) on tamarack C_i/C_{a750} as increasing growth temperature led to increased C_i/C_{a750}, but no significant growth treatment effects ($p > 0.24$ for all; Figure 3.17 and D, Table 2). Again, there was a strong measurement temperature effect ($p < 0.0001$) as C_i/C_{a750} decreased from 10 °C to 25 °C then increased again up to 40 °C.
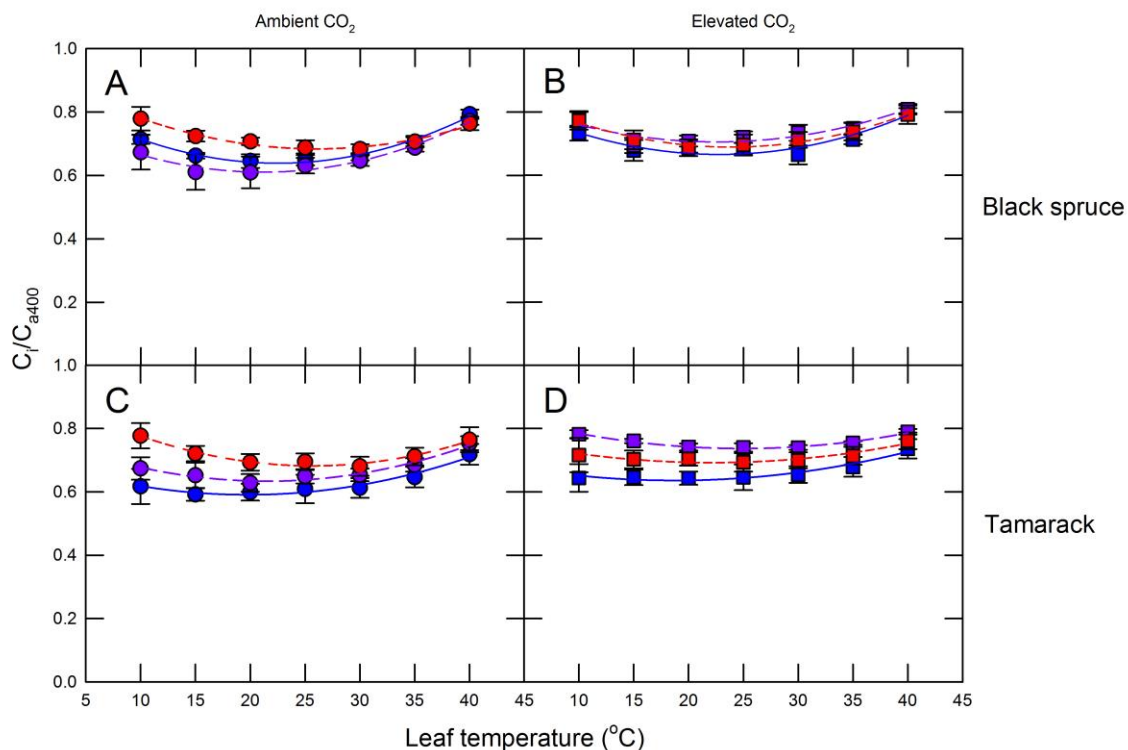
Figure 3.6 Ratio of intercellular CO_2 concentration to ambient CO_2 concentration (C_i/C_{a400}) of black spruce and tamarack measured at 400 ppm CO_2.

Measurements were taken at a saturating light level of 1400 μmol photons m^{-2} s^{-1}. Data shown as means ± SE, n = 5. Blue symbols and solid lines represent ambient temperature seedlings (T0), purple symbols and long-dashed lines represent +4 °C-warmed seedlings (T4), and red symbols and short-dashed lines represent +8 °C-warmed seedlings (8T). Circles represent ambient CO_2 growth conditions of 400 ppm (AC), squares represent elevated CO_2 growth conditions of 750 ppm CO_2 (EC).
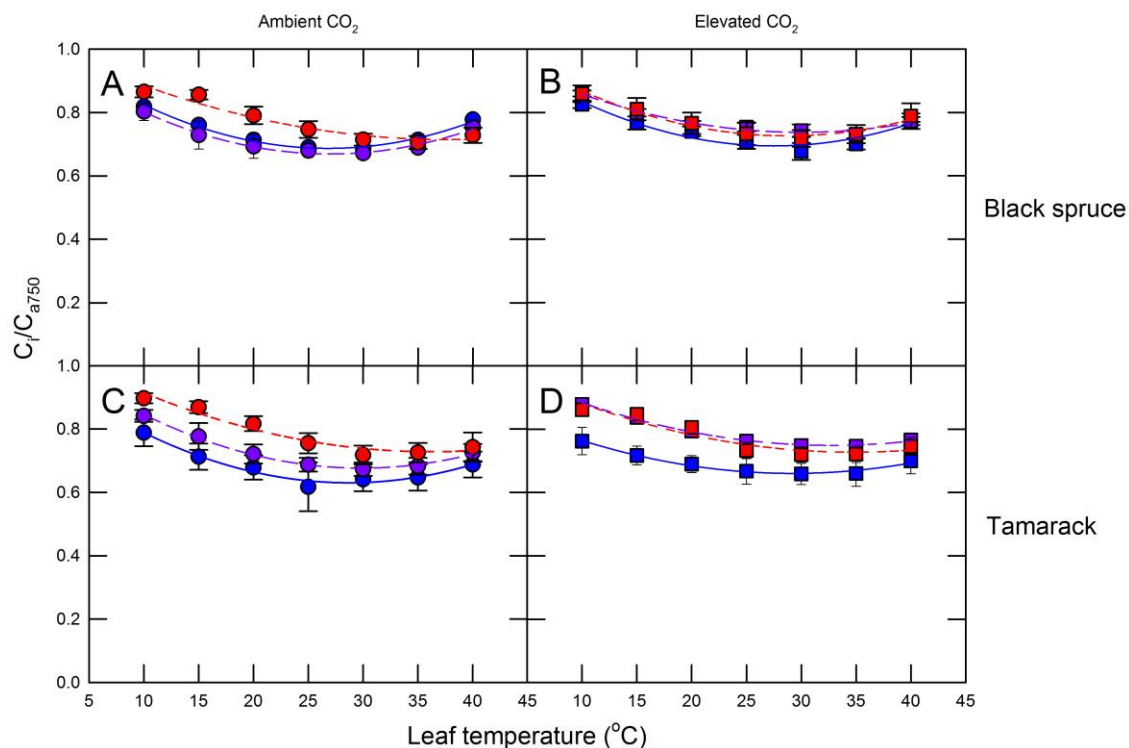
Figure 3.7 Ratio of intercellular CO_2 concentration to ambient CO2 concentration (C_i/C_{a750}) of black spruce and tamarack measured at 750 ppm CO_2.

Measurements were taken at a saturating light level of 1400 μmol photons m^{-2} s^{-1}. Data shown as means ± SE, n = 5. Blue symbols and solid lines represent ambient temperature seedlings (T0), purple symbols and long-dashed lines represent +4 °C-warmed seedlings (T4), and red symbols and short-dashed lines represent +8 °C-warmed seedlings (8T). Circles represent ambient CO_2 growth conditions of 400 ppm (AC), squares represent elevated CO_2 growth conditions of 750 ppm CO_2 (EC).

3.4 Photosynthetic thermal optima responses to growth temperature and CO_2

3.4.1 Black spruce

The thermal optima of both A_{400} and A_{750} (T_{opt400} and T_{opt750}, respectively) increased significantly as growth temperature increased ($p < 0.0025$; Figures 3.8A and 3.9A; Table 3). ACT8-grown trees had a 13.3 % higher T_{opt400} and a 15.4 % higher T_{opt750} than ACT0 trees, while T_{opt} increased 11.3% for the same 8 °C increase in growth temperature in the EC seedlings in both measurement CO_2 concentrations. At neither measurement CO_2 did spruce show a significant T_{opt} response to growth CO_2 conditions, nor was there a significant interaction between growth CO_2 and temperature on T_{opt} (Table 3).

3.4.2 Tamarack

Tamarack T_{opt} (measured at both 400 and 750 ppm CO_2) increased with increasing growth temperature ($p < 0.021$; Figures 3.8B and 3.9B; Table 3). ACT8 trees had an 18.9 % higher T_{opt400} and a 19.2% higher T_{opt750} than ACT0 trees; in the EC treatment, T_{opt400} increased by 15.9% in the ECT8 seedlings compared to the ECT0 trees and T_{opt750} increased by 20.7 % (Figures 3.8B and 3.9B). At neither measurement CO_2 did tamarack show a significant T_{opt} response to growth CO_2, nor was there a significant interaction between growth CO_2 and growth temperature on T_{opt} (Table 3).
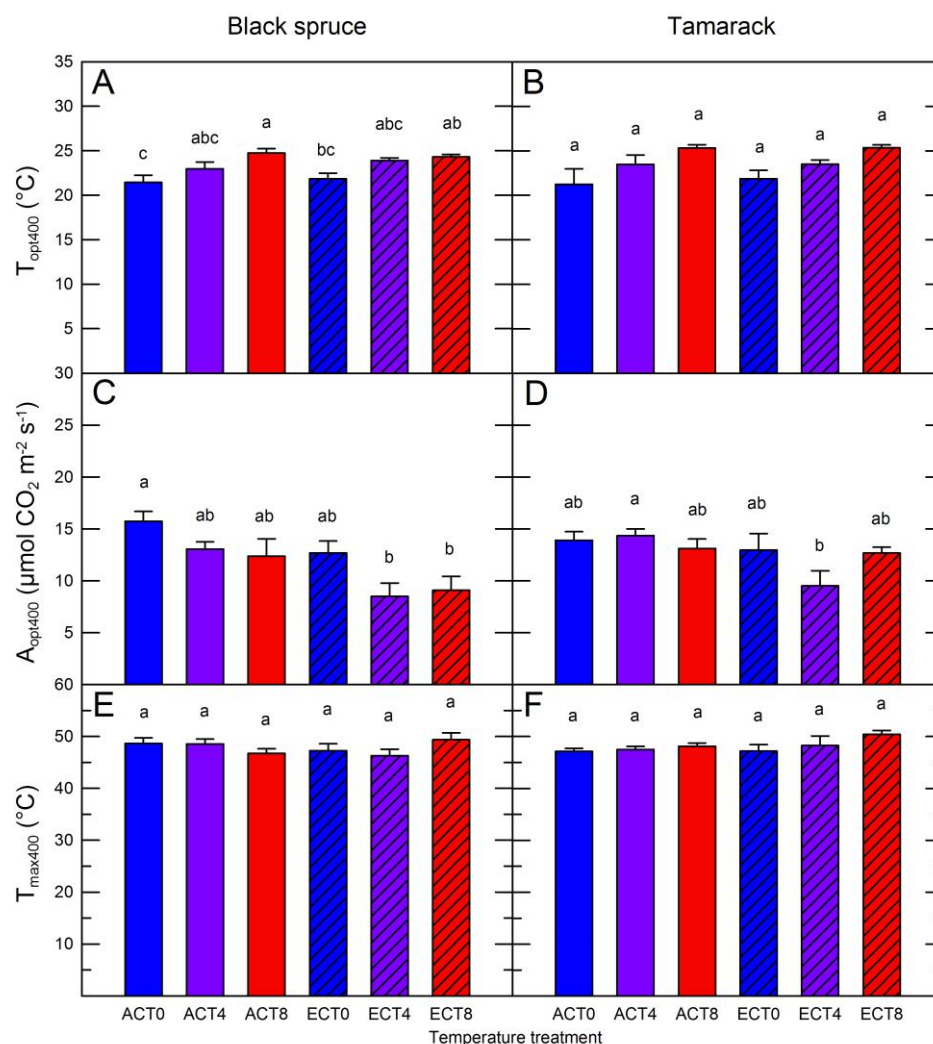
Figure 3.8 Photosynthetic thermal optimum (T_{opt400}), maximum rate of net CO_2 assimilation (A_{opt400}), and high temperature CO_2 compensation point (T_{max400}) of black spruce and tamarack.

Measurements were taken at a saturating light level of 1400 μmol photons m^{-2} s^{-1} and a measurement CO_2 of 400 ppm. Data shown as means ± SE, n = 5. Blue bars represent ambient temperature seedlings, purple bars represent +4 °C-warmed seedlings, and red bars represent +8 °C-warmed seedlings. Solid bars represent ambient CO_2 growth conditions of 400 ppm (AC), hashed bars represent elevated CO_2 growth conditions of 750 ppm CO_2 (EC). Different letters above bars denote a significant difference (p < 0.05).
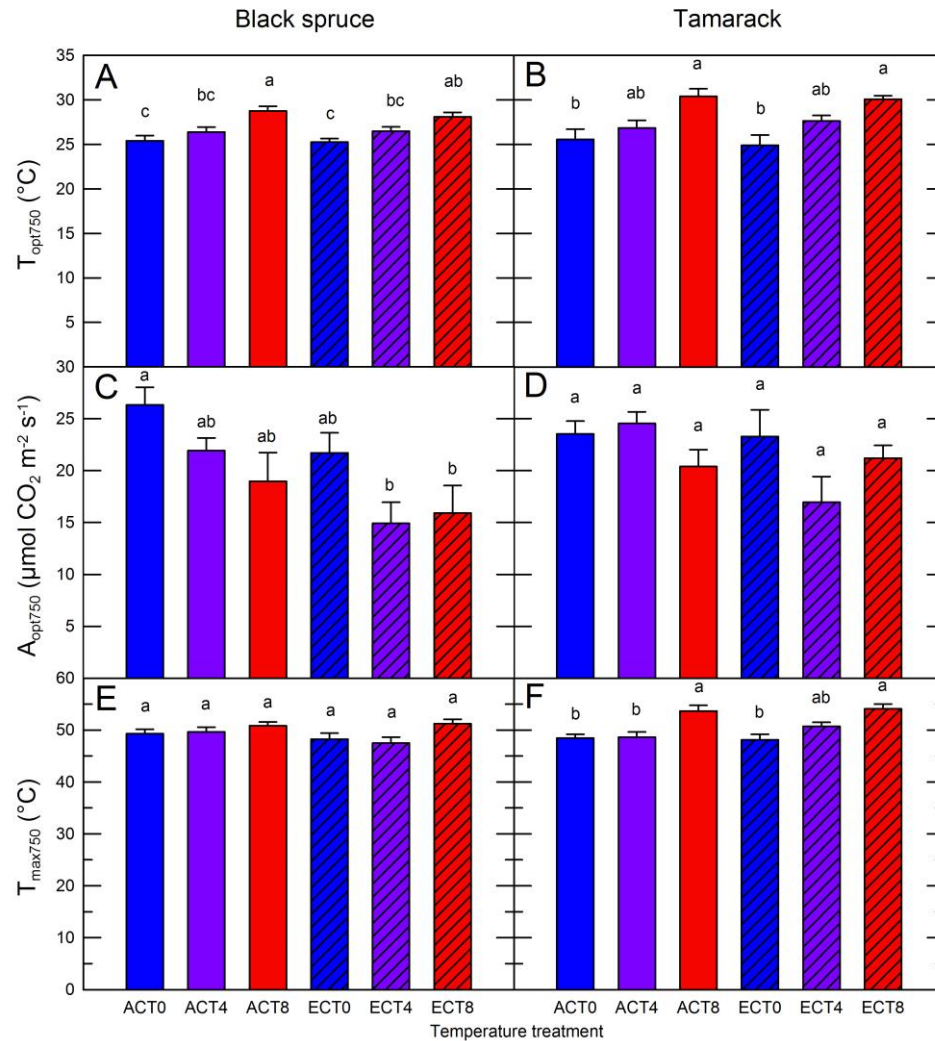
Figure 3.9 Photosynthetic thermal optimum (T_{opt750}), maximum rate of net CO_2 assimilation (A_{opt750}), and high temperature CO_2 compensation point (T_{max750}) of black spruce and tamarack.

Measurements were taken at a saturating light level of 1400 μmol photons m^{-2} s^{-1} and a measurement CO_2 of 750 ppm. Data shown as means $\pm$ SE, n = 5. Blue bars represent ambient temperature seedlings, purple bars represent +4 °C-warmed seedlings, and red bars represent +8 °C-warmed seedlings. Solid bars represent ambient CO_2 growth conditions of 400 ppm (AC), hashed bars represent elevated CO_2 growth conditions of 750 ppm CO_2 (EC). Different letters above bars denote a significant difference (p < 0.05).

Table 3 Summary ANOVA statistics table for black spruce and tamarack respiratory and photosynthetic characterizations of Q_{10}, photosynthetic thermal optimum measured at 400 ppm CO_2 (T_{opt400}), photosynthetic thermal optimum measured at 750 ppm CO_2 (T_{opt750}), maximal rate of net CO_2 assimilation measured at 400 ppm CO_2 (A_{opt400}), maximal rate of net CO_2 assimilation measured at 750 ppm CO_2 (A_{opt750}), maximal temperature of net CO_2 assimilation measured at 400 ppm CO_2 (T_{max400}), and maximal temperature of net CO_2 assimilation measured at 750 ppm CO_2 (T_{max750}).

Bolded p values are statistically significant ($p < 0.05$), italicized p values represent $0.10 \geq p \geq 0.05$. T = growth temperature treatment, CO_2 = growth CO_2 concentration, and T_m = measurement leaf temperature.

	Black spruce	**Tamarack**	**DF**
T_{opt400}			
CO_2	0.64	0.65	1
T	**0.003**	**0.021**	2
T × CO_2	0.52	0.94	2
T_{opt750}			
CO_2	0.84	0.59	1
T	**0.0003**	**0.002**	2
T × CO_2	0.75	0.69	2
A_{opt400}			
CO_2	*0.088*	0.54	1
T	0.14	0.72	2
T × CO_2	0.81	0.10	2
A_{opt750}			
CO_2	0.14	0.93	1
T	*0.066*	0.29	2
T × CO_2	0.65	*0.076*	2
T_{max400}			
CO_2	0.39	0.81	1
T	0.42	0.98	2
T × CO_2	*0.091*	0.55	2
T_{max750}			
CO_2	0.44	0.80	1
T	0.50	**0.00094**	2
T × CO_2	0.42	0.46	2

Spruce A_{opt400} did not respond to warming (p = 0.14; Figure 3.8C; Table 3). Although, spruce A_{opt400} did tend to decrease at increased growth CO_2 (p = 0.088), with the average EC A_{opt} (across all temperature treatments) being 26.5 % lower than that of all AC-grown trees. There was also a trend of A_{opt750} decreasing with increasing growth temperature (p = 0.066; Figure 3.9C, Table 3). A_{opt750} decreased by 27 % from T0 to T8-grown trees in both CO_2 treatments. There were no significant interactions between growth temperature and growth CO_2 on any spruce A_{opt} (Table 3).

Tamarack A_{opt400} did not show any response to growth CO_2 or growth temperature (Figure 3.8D, Table 3) – there were also no significant effects of growth temperature or CO_2 on tamarack A_{opt750} (Figure 3.9D, Table 3). There was no interaction between growth CO_2 and growth temperature in A_{opt400} in tamarack. However, there was a statistical trend for an interaction between growth temperature and growth CO_2 for A_{opt750} in tamarack (p = 0.076): as ECT4 seedlings tended to have a lower A_{opt750} than ACT4 seedlings (Figure 3.9D, Table 3). The A_{opt400} of ECT4 tamaracks was 26.6 % lower than that of ECT0 trees and 33.2 % lower than ECT8 trees (Figure 3.9D). The A_{opt750} of ECT4 tamaracks was 27.2 % lower than ECT0 trees and 25.1 % lower than trees grown in the ECT8 treatment (Figure 3.9D).

When measured at either 400 or 750 ppm CO_2, T_{max} did not respond to growth temperature or CO_2 in spruce (p > 0.39 for all; Figures 3.8E and 3.9E, Table 3). There was, however, a trend suggesting an interaction of growth temperature and CO_2 for

T_{max400} (p = 0.091), as T_{max400} in ECT8 seedlings was slightly higher than in ACT8

spruce. There was no significant interaction between growth CO_2 and temperature for

spruce T_{max750} (Table 3). T_{max400} in tamarack did not respond to growth temperature,

growth CO_2, nor was there an interaction between the two (p > 0.55 for all; Figure 3.8F,

Table 3). The T_{max750} increased with increasing growth temperature in tamarack (p =

0.00094), but there was no growth CO_2 effect (p = 0.46) nor an interaction between

growth CO_2 and temperature (p = 0.80; Figure 3.9F, Table 3).

3.5 Respiratory response to growth temperature and CO_2

3.5.1 Black spruce

Elevated growth temperature conditions significantly decreased spruce R_{dark} (p = 0.01)

but growth CO_2 did not have an effect (p = 0.85) (Figure 3.10A and B, Table 4).

Measurement temperature significantly affected spruce R_{dark} (p < 0.0001), as the expected

stimulation of R_{dark} was observed as measurement temperature increase. There was no

interaction between growth temperature and growth CO_2 on spruce R_{dark} (p = 0.099) nor

between measurement temperature and growth CO_2 (p = 0.17, Table 4). There was a

significant interaction between measurement temperature and growth temperature (p =

0.038; Table 4) as increasing growth temperatures resulted in lower rates of R_{dark} across

the measurement temperature range. There was also a trend of an interaction among

measurement temperature, growth temperature, and growth CO_2 (p = 0.059), such that

ECT4 and ECT8 trees showed slightly lower R_{dark} than ACT4 and ACT0 trees,

respectively (Figure 3.10A and B).
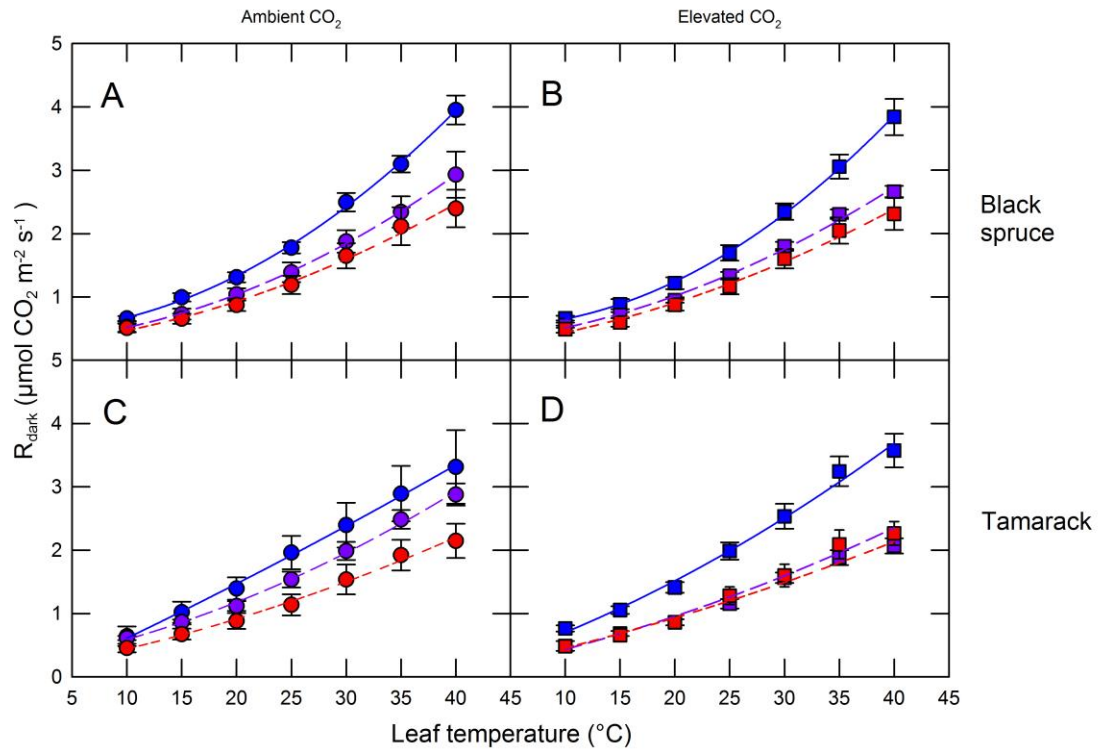
Figure 3.10 Dark respiration (R_{dark}) of black spruce and tamarack.

Measurements were taken between 10 °C and 40 °C at a light level of 0 μmol photons m^{-2} s^{-1} and a measurement CO_2 of 400 ppm. Data shown as means ± SE, n = 5. Blue symbols and solid lines represent ambient temperature seedlings (T0), purple symbols and long-dashed lines represent +4 °C-warmed seedlings (T4), and red symbols and short-dashed lines represent +8 °C-warmed seedlings (8T). Circles represent ambient CO_2 growth conditions of 400 ppm (AC), squares represent elevated CO_2 growth conditions of 750 ppm CO_2 (EC).

Table 4 Summary ANOVA statistics table for black spruce and tamarack respiratory parameters of dark respiration (R_{dark}), thermal sensitivity of R_{dark} (Q_{10}), dark respiration measured at a fixed temperature of 25 °C (R_{dark25}).

Bolded p values are statistically significant ($p < 0.05$), italicized p values represent $0.10 \geq p \geq 0.05$. T = growth temperature treatment, CO_2 = growth CO_2 concentration, and T_m = measurement leaf temperature.

	Black spruce	**Tamarack**	**DF**
R_{dark}			
CO_2	0.85	0.68	1
T	0.01	**0.045**	2
T_m	**<0.0001**	**0.0001**	6
$T \times CO_2$	*0.099*	0.35	2
$T_m \times CO_2$	0.17	0.21	6
$T_m \times T$	**0.038**	0.19	12
$T_m \times CO_2 \times T$	*0.059*	0.28	12
Q_{10} (10-40 °C)			
CO_2	0.66	0.32	1
T	**0.018**	0.53	2
$T \times CO_2$	0.25	0.55	2
R_{dark25}			
CO_2	0.62	0.96	1
T	**0.015**	**0.012**	2
$T \times CO_2$	0.95	0.42	2

3.5.2 Tamarack

Growth CO_2 conditions did not have a significant effect on tamarack R_{dark} (p = 0.68); however, there was a significant effect of growth temperature (p = 0.045), such that needles grown at warmer temperatures had lower rates of R_{dark} (Figure 3.10C and D, Table 4). Measurement temperature significantly affected tamarack R_{dark} (p = 0.0001) as it did in spruce. There was no significant interaction between growth temperature and growth CO_2 on tamarack R_{dark}, nor between measurement temperature and growth CO_2, measurement temperature and growth temperature, nor between measurement temperature, growth temperature, and growth CO_2 (p > 0.19 for all; Table 4).

3.5.3 Respiratory Q_{10}

When the Q_{10} was calculated across the entire leaf measurement temperature range (10-40 °C), there was a significant effect of growth temperature in spruce (p = 0.018; Figure 3.11A, Table 4), as the Q_{10} in spruce decreased with increasing growth temperatures. There was no significant growth CO_2 effect nor an interaction between growth temperature and CO_2 in the Q_{10} from 10-40 °C in spruce. There were no significant effects of growth temperature, growth CO_2, nor growth treatment interactions on tamarack Q_{10} calculated over the 10-40 °C range (p ≥ 0.32 for all; Figure 3.11B, Table 4).
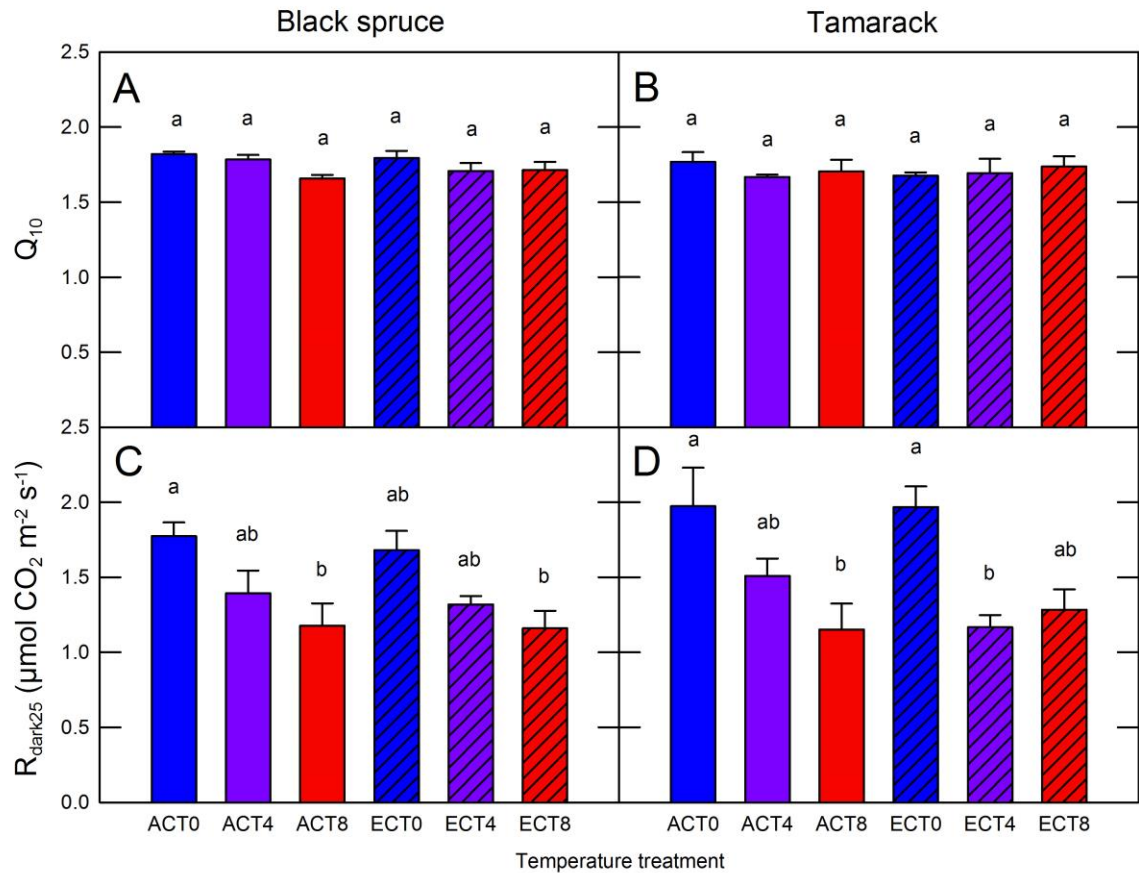
Figure 3.11 Respiratory Q_{10} (over the 10-40 °C measurement range) and dark respiration rate at a fixed measurement temperature of 25 °C (R_{dark25}) of black spruce and tamarack.

Measurements were taken at a light level of 0 μmol photons m^{-2} s^{-1} and a measurement CO_2 of 400 ppm. Data shown as means ± SE, n = 5. Blue bars represent ambient temperature seedlings, purple bars represent +4 °C-warmed seedlings, and red bars represent +8 °C-warmed seedlings. Solid bars represent ambient CO_2 growth conditions of 400 ppm (AC), hashed bars represent elevated CO_2 growth conditions of 750 ppm CO_2 (EC). Different letters above bars denote a significant difference (p < 0.05).

3.5.4 R_{dark} at 25 °C

When R_{dark} was measured at a common leaf temperature of 25 °C (R_{dark25}), both black spruce (p = 0.015) and tamarack (p = 0.012) R_{dark25} decreased with increasing growth temperature (Figure 3.11C and D, Table 4). There were no growth CO_2 effects on either species, nor any interactions (Table 4).

3.6 Response of tree growth to elevated temperature and CO_2

Elevated growth CO_2 increased black spruce height by 21.4 % compared to AC seedlings (p < 0.0001; Figure 3.12A, Table 4). There was also a trend for reduced shoot height in spruce with increasing temperature (p = 0.069). There was a significant temperature effect on tamarack height (p = 0.0012; Table 4); trees were tallest in the T4 treatment in both growth CO_2 concentrations (Figure 3.12B). There was a trend of a CO_2 enrichment effect increasing tamarack height (p = 0.054): ECT0 trees were 15.9 % taller than those grown in ACT0 conditions. There was no significant interaction between CO_2 and temperature on shoot height in either species (Table 4).

Growth temperature had a significant effect on spruce stem diameter: extreme warming significantly reduced stem diameter in the T8 treatment at both growth CO_2 concentrations compared to the T0 and T4 treatments (p = 0.00074; Figure 3.12C, Table 4). Stem diameter was 20.7% and 28.3 % smaller in T8 spruce than in T0 spruce in AC and EC-grown spruce, respectively. Elevated growth CO_2 increased black spruce stem diameter (p = 0.00020). There was also a trend for an interaction between growth CO_2
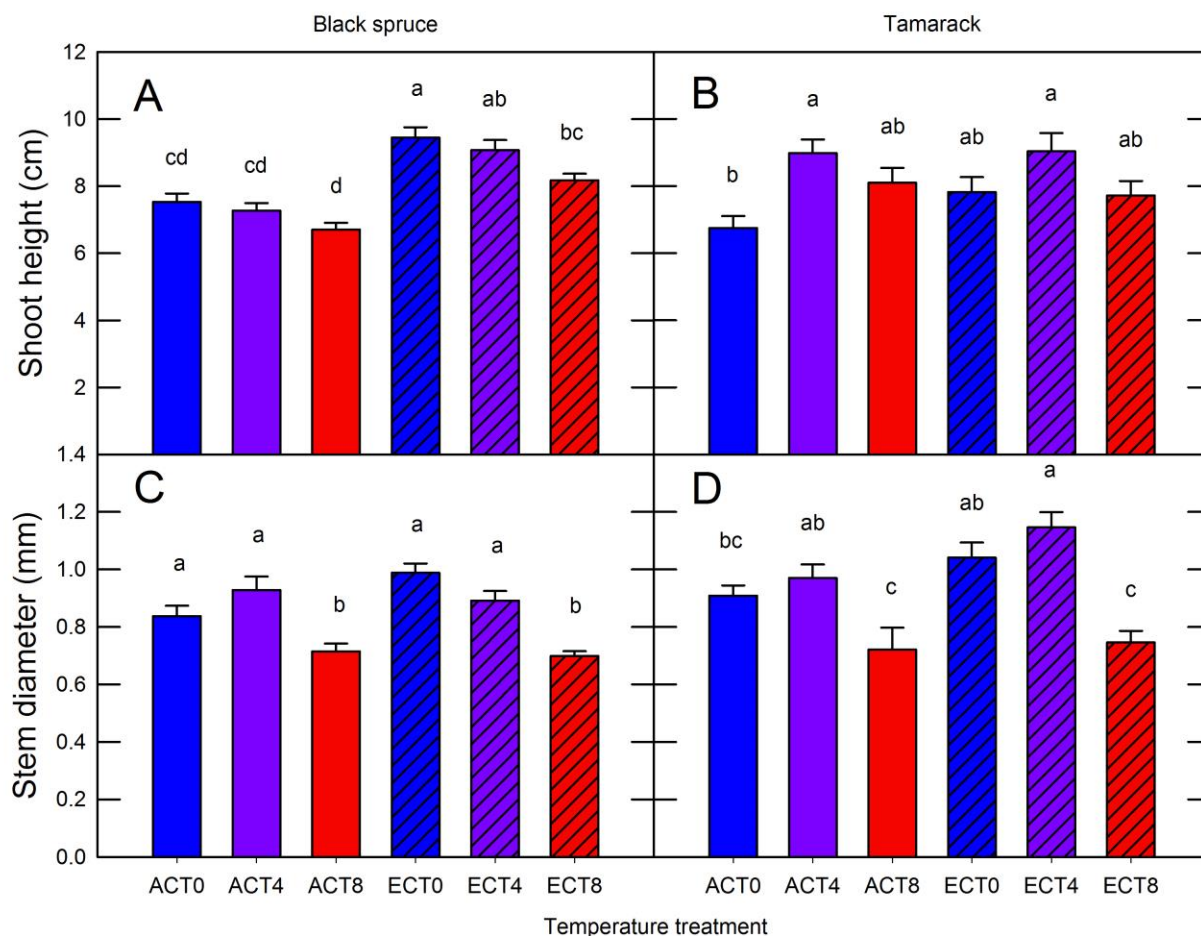
Figure 3.12 Shoot height and stem diameter of black spruce and tamarack.

Data shown as means ± SE, n = 5. Blue bars represent ambient temperature seedlings, purple bars represent +4 °C-warmed seedlings, and red bars represent +8 °C-warmed seedlings. Solid bars represent ambient CO_2 growth conditions of 400 ppm (AC), hashed bars represent elevated CO_2 growth conditions of 750 ppm CO_2 (EC). Different letters above bars denote a significant difference ($p < 0.05$).

Table 5 Summary ANOVA statistics table for black spruce and tamarack and anatomical parameters of shoot height, stem diameter, % N, and leaf mass per unit area (LMA).

Bolded p values are statistically significant ($p < 0.05$), italicized p values represent $0.10 \geq p \geq 0.05$. T = growth temperature treatment, CO_2 = growth CO_2 concentration, and T_m = measurement leaf temperature.

	Black spruce	Tamarack	DF
Shoot height			
CO_2	**<0.0001**	*0.054*	1
T	*0.069*	**0.0012**	2
$T \times CO_2$	0.65	0.22	2
Stem diameter			
CO_2	**0.00020**	0.67	1
T	**0.00074**	**0.00063**	2
$T \times CO_2$	*0.088*	0.64	2
% N			
CO_2	0.35	0.29	1
T	**0.0008**	**0.019**	2
$T \times CO_2$	**0.0021**	*0.072*	2
LMA			
CO_2	0.46	0.85	1
T	0.24	**0.0088**	2
$T \times CO_2$	*0.097*	0.41	2

and T (p = 0.09), such that spruce seedlings had a larger stem diameter in the ECT0 treatment compared to the ACT0 trees.

Tamarack stem diameter showed a significant response to growth temperature (p = 0.00063), but not growth CO_2 (p = 0.67), with the lowest stem diameter occurring in 8T seedlings at both growth CO_2 conditions (Figure 3.12D, Table 4). There was no interaction between CO_2 and temperature on stem diameter in tamarack (Table 4).

3.7 Percent nitrogen and leaf mass per unit area (LMA)

Growth temperature significantly reduced leaf % N in spruce (p = 0.0008; Figure 3.13, Table 4), but growth CO_2 had no effect on spruce needle nitrogen content. There was a significant interaction between growth temperature and growth CO_2 on leaf % N in spruce (p = 0.002), such that T4 % N was the lowest of the three EC temperature treatments, but T8 was the lowest % N in the AC treatments. Tamarack responded to growth treatments in much the same way as spruce; increasing growth temperatures decreased leaf % N (p = 0.02; Figure 3.13, Table 4) and growth CO_2 did not have a significant effect on leaf % N (p = 0.29). There was a statistical trend of an interaction between growth temperature and growth CO_2 on leaf % N in tamarack, such that ECT4 % N was the lowest of the three EC temperature treatments, whereas in the AC treatment, % N decreased in order of increasing growth temperature (p = 0.07).
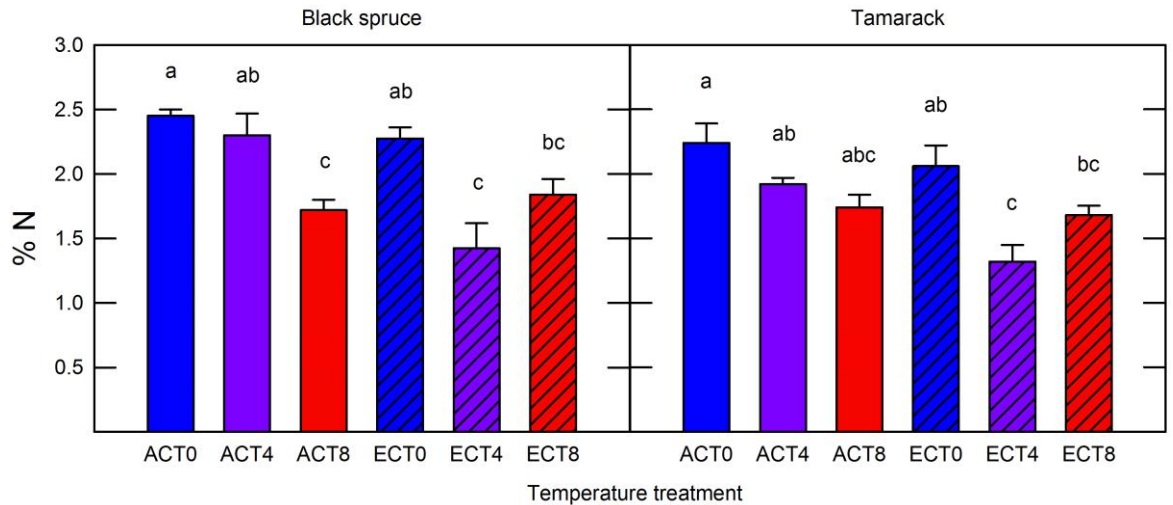
Figure 3.13 Needle percent nitrogen and carbon content of black spruce and tamarack.

Data shown as means ± SE, n = 5. Blue bars represent ambient temperature seedlings, purple bars represent +4 °C-warmed seedlings, and red bars represent +8 °C-warmed seedlings. Solid bars represent ambient CO_2 growth conditions of 400 ppm (AC), hashed bars represent elevated CO_2 growth conditions of 750 ppm CO_2 (EC). Different letters above bars denote a significant difference ($p < 0.05$).

Black spruce LMA did not respond significantly to growth temperature ($p = 0.24$) or growth CO_2 ($p = 0.46$); however, there was a statistical trend for an interaction between growth temperature and CO_2 as LMA was highest in the T0 treatment at AC, but in the T4 treatment at EC ($p = 0.097$; Figure 3.14A, Table 4). Tamarack LMA decreased significantly with increasing growth temperature ($p = 0.0089$) but did not respond to growth CO_2 ($p = 0.85$); there was no significant interaction between growth temperature and growth CO_2 ($p = 0.41$; Figure 3.14B, Table 4).
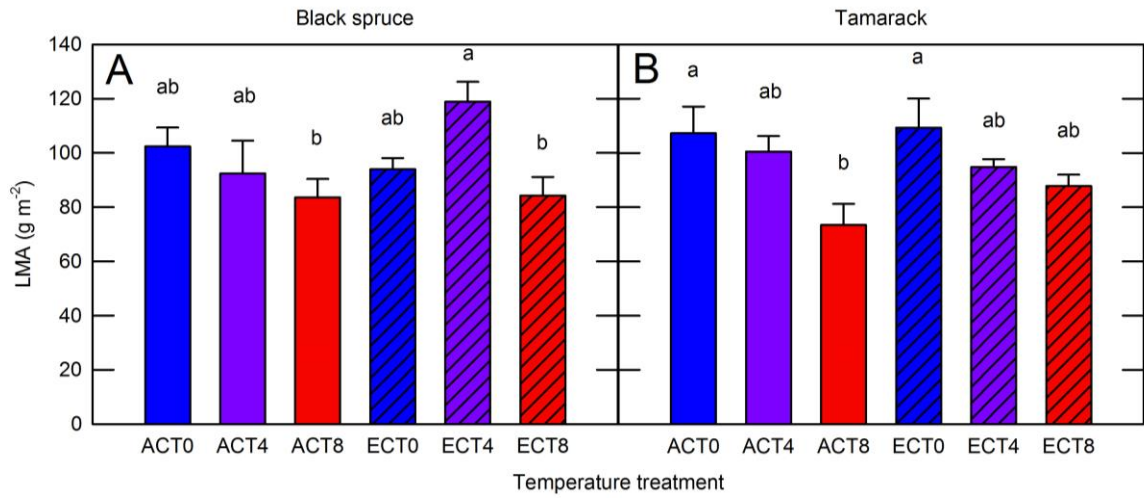
Figure 3.14 Leaf mass per unit area (LMA) of black spruce and tamarack.

Data shown as means ± SE, n = 5. Blue bars represent ambient temperature seedlings, purple bars represent +4 °C-warmed seedlings, and red bars represent +8 °C-warmed seedlings. Empty bars represent ambient CO_2 growth conditions of 400 ppm, hashed bars represent elevated CO_2 growth conditions of 750 ppm CO_2.

Chapter 4: Discussion

4.1 The future of black spruce and tamarack in the boreal forest

Black spruce acclimated net photosynthesis to warming with primarily detractive adjustments, demonstrating that the physiology of the seedlings used in this experiment was best suited to current, ambient conditions and higher temperatures impair net carbon gain. Spruce was effective at acclimating respiratory losses to increased growing temperatures; however, shoot height and stem diameter decreased in the warmer treatments, suggesting that aboveground carbon sequestration will be weakened in future warming scenarios despite acclimating R_{dark}. While the detrimental effects of moderate warming on spruce stem diameter were fully mitigated by enriched growth CO_2, extreme warming still caused a significant reduction in stem diameter regardless of growth CO_2 treatment.

Tamarack, on the other hand, did not acclimate A_{net} to increasing temperatures; instead, net carbon gain remained constant across temperature treatments. However, when measured at 750 ppm CO_2, extreme warming decreased rates of A_{net}. Tamarack seedlings acclimated R_{dark} to a lesser extent than spruce; however, increased aboveground biomass allocation with moderate warming may have required higher rates of growth respiration. Tamarack height and stem diameter increased with 4 degree warming and declined considerably with 8 degree warming, suggesting that seedlings may benefit from projected mid-century climates where spruce, ostensibly, will not.

Declining foliar nitrogen concentration underpinned the acclimation of A_{net} and R_{dark} in black spruce and tamarack. Photosynthetic enzymes and pigments are the largest nitrogen pools in leaves (Sage and Pearcy, 1987) and low leaf N usually translates into low photosynthetic capacity, such that the biochemical demand for CO_2 is reduced. As the seedlings of this experiment were well fertilized, changes in leaf nitrogen were not likely due to poor supply. But if both species had reduced leaf N and reduced photosynthetic capacity (which is corroborated by unpublished data from these same trees), how could tamarack maintain high rates of A_{net}? The answer likely lies in the ability to supply CO_2 to the site of carboxylation. Whereas spruce stomatal conductance (g_s) was lowest in warm-grown trees, tamarack appeared to mitigate the effects of low foliar nitrogen in warm-grown trees by increasing g_s, which would increase CO_2 substrate availability to the Calvin Cycle, thereby boosting A_{net}. The fundamental differences in acclimation of carbon dynamics between the two species became manifest in their accumulation of aboveground biomass, where spruce aboveground biomass responded negatively in all warming scenarios whereas tamarack increased height and diameter with 4 degree warming.

While the reality of field experiments is quite different than the highly-controlled laboratory setting of my experiment, the physiological limitations of spruce A_{net} in response to warming suggest that future climates will impair the ability of this species to compete in the boreal forest. Tamarack may become a more dominant species in the

future, as the predicted temperature and CO_2 conditions of coming decades exceed the ability of black spruce to acclimate carbon gain.

4.2 Thermal acclimation of A_{net} in black spruce and tamarack

4.2.1 Black spruce

Under no circumstances did spruce A_{net} improve at high measurement temperatures when grown in warm conditions. Thermal acclimation of A_{net} occurred; however, all adjustments were detractive. Moreover, rates of A_{net} in warm-grown trees were consistently lower at low measurement temperatures, indicating that T4 and T8 warming regimes reduced net photosynthetic carbon gain in spruce relative to trees grown in current thermal conditions. The limited acclimation potential of black spruce therefore appears to be insufficient for the species to maintain photosynthetic homeostasis at moderate and extreme warming scenarios, let alone improve net photosynthetic efficiency relative to seedlings grown in current, ambient conditions. Previous studies with black spruce have found similar limitations of A_{net} in high temperature-grown trees, also attributed to lower leaf nitrogen concentrations (Way and Sage 2008a, 2008b).

Black spruce T_{opt} increased with growing temperature in both ambient and elevated CO_2-grown seedlings at both measurement CO_2 concentrations, indicating a partial degree of thermal acclimation (Way and Sage 2008a, Way and Yamori 2014). However, spruce A_{opt} (the maximum rate of carbon assimilation at T_{opt}) was lower in warm-grown treatments, meaning that warm-grown trees still had lower carbon gain relative to cool-

grown trees. As well, the T_{max} of A_{net} (where photosynthetic carbon gain and respiratory carbon loss are in equilibrium) should shift to a higher temperature in a warm-acclimated plant, such that carbon gain at higher measurement temperatures is improved relative to a cool-acclimated plant (Yamori et al. 2014), but warm-grown black spruce seedlings did not have increased T_{max}, Taken together, the data indicate little plasticity in spruce for A_{net} to acclimate to increasing growth temperatures.

4.2.2 Tamarack

Tamarack, on the other hand, showed no significant acclimation of A_{400} to temperature, indicating that net carbon gain was not sensitive to increases in growth temperature. This is consistent with previous research on thermal acclimation of A_{net} in tamarack seedlings (Tjoelker et al. 1998). At A_{750}, there was evidence of constructive adjustment of A_{net}, as T_{max} increased with moderate warming, although T8 trees had lower A_{net} compared to T0 trees. A_{opt} also tended to be lower in T8 than T0 tamarack seedlings, which would suggest that extreme warming impaired A_{net}, but a larger sample size may be required to demonstrate a statistical significance for this effect. The degree of thermal acclimation of carbon assimilation was most clear in the A_{750} curves, where the higher A_{net} rates allow for greater separation of the data. ACT4 seedlings showed a classic thermal acclimation response as rates of A_{750} were slightly higher than ACT0 at higher measurement temperatures. ACT8 seedlings had lower rates of A_{750} compared to ACT0 seedlings at all but the highest measurement temperatures, at which point they were commensurate with the A_{750} rates of ACT0. These results suggest that tamarack responses to moderate (T4) warming may lead to improvements in A_{net}, or at the very least, moderate warming does

not reduce A_{net}, while extreme warming (T8) of tamarack seedlings results in diminished net photosynthesis. As with black spruce, tamarack T_{opt} increased with increasing growth temperature and the A_{opt750} remained constant among all temperature treatments, indicating a constructive adjustment in net carbon assimilation.

Interestingly, A_{net} was lower in ECT4 spruce and tamarack then in either ECT0 or ECT8. This "anomaly" is, however, underpinned by lower leaf nitrogen concentration ECT4 leaves of both species. Investment in photosynthetic apparatus is directly influenced by leaf nitrogen concentration (Warren et al. 2003, Way and Sage 2008a, Scafaro et al. 2016) so the low A_{net} in the ECT4 treatment is likely attributable to the low needle nitrogen concentration.

4.3 CO_2 acclimation of A_{net} in black spruce and tamarack

In black spruce, A_{net} showed significant acclimation to CO_2: A_{net} was lower in EC-grown trees at all growth temperatures compared to AC-grown trees, when measured at a common CO_2 concentration (either A_{400} or A_{750}). Photosynthetic down-regulation has been found before in black spruce seedlings grown at high CO_2 and was found to be a result of decreased photosynthetic capacity (Tjoelker et al. 1998). When A_{net} was assessed at growth CO_2 conditions (A_{growth}), net carbon assimilation was higher in EC-grown trees, likely as the instantaneous effect of high measurement CO_2 allowed for high levels of substrate availability for CO_2 fixation in EC trees (Crous et al. 2008). Growth

CO_2 did not have any effect on spruce T_{opt}; however, there was a trend of decreased A_{opt400} in EC-grown spruce seedlings, supporting the finding of CO_2 acclimation of A_{net}.

Unlike black spruce, tamarack did not acclimate to elevated growth CO_2 conditions, and EC-grown trees did not show a down-regulation of A_{net} compared to AC-grown trees. This is contrary to previous results which have found acclimation of A_{net} in elevated CO_2-grown tamarack (Tjoelker et al. 1998). This difference could be attributed to the small pot size used by Tjoelker *et al.* (1998) which would limit seedling growth and therefore carbohydrate sink demand. The only exception to this was the unusual suppression of A_{net} in ECT4 trees at both A_{400} and A_{750} mentioned earlier. There were no effects of growth CO_2 on T_{opt} or A_{opt} (save for a decreased A_{opt750} in the ECT4 treatment as discussed previously). The lack of CO_2 acclimation in tamarack may be indicative of an absence of carbohydrate sink limitations in high CO_2-grown seedlings conditions (Moore et al. 1999, Ainsworth and Rogers 2007, Lemoine et al. 2013), which may be linked to the higher growth of tamarack seedlings in EC (Coleman et al. 2008), demonstrating a notable difference between black spruce and tamarack response to elevated growth CO_2.

4.4 Stomatal conductance and intercellular CO_2 ratio response to elevated temperature and CO_2

Stomatal conductance (g_s) was consistently highest in T0 spruce in both ambient and elevated growth CO_2 conditions and at both measurement CO_2 concentrations. Measurement CO_2 did not influence spruce g_s, suggesting that stomatal conductance was not responsive to acute changes in ambient CO_2. This result is consistent with previous

research characterizing conifer species as having a conservative, insensitive stomatal response to changes in ambient CO_2 compared to broad-leaved species (Tjoelker et al. 1999a, Medlyn et al. 2001). At both measurement CO_2 concentrations, g_s was suppressed in EC-grown spruce, indicating acclimation of g_s to high-CO_2 growing conditions. Acclimation of g_s to elevated CO_2 has been found across several tree species (reviewed in Medlyn et al. 2001). Suppressed g_s in EC-grown spruces is consistent with the suppressed A_{net} curves of the same trees, potentially implying a causal effect of stomatal limitations on A_{net} reduction seen in EC trees.

Tamarack g_s was not significantly influenced by growth temperature or growth CO_2 concentration; however, an apparent stratification of g_s by growth temperatures is visible, suggesting increased g_s with increasing growth temperatures. A larger sample size may have been able to detect a growth temperature effect on g_s if it exists; however, higher g_s in warm-grown trees would certainly explain the constructive adjustments of A_{net} seen in tamarack.

The ratio of intracellular CO_2 (C_i) to ambient CO_2 (C_a) represents the balance of CO_2 diffusing into the leaf and CO being fixed by Rubisco. If a plant's CO_2 intake is not commensurate with its rate of CO_2 fixation, the former becomes a constraint on A_{net} (Farquhar et al. 1980). None of the growth treatments induced significant changes in C_i/C_a for spruce, suggesting that reduced g_s limiting CO_2 supply to photosynthesis was balanced by a reduced biochemical ability to fix CO_2. Tamarack C_i/C_a, however, showed

an increasing trend matching the stratification of g_s whereby C_i/C_a increased with increasing growth temperature. This suggests that diminishing biochemical demand for CO_2 in photosynthesis was mitigated in tamarack by increasing substrate supply.

4.5 Acclimation of R_{dark} to elevated temperature and CO_2

Black spruce showed strong thermal acclimation of R_{dark}; rates of R_{dark} decreased with increasing growth temperature. While average air temperature in the Canadian boreal could warm by up to 8 °C by 2100 (IPCC, 2014), leaf temperatures have been shown to exceed air temperature by more than 6 °C (Martin et al. 1999). Therefore, acclimation of R_{dark} at high measurement temperatures is central to maintaining a positive carbon balance. The significant reduction in spruce R_{dark25} with increasing growth temperature obviates a reduced slope of the R/T curve and is consequently strong evidence of Type I respiratory acclimation (Atkin and Tjoelker 2003).

Like spruce, tamarack seedlings acclimated R_{dark} to temperature such that warm-grown trees maintained lower rates of R_{dark} than cool-grown trees. While spruce showed a discernible stratification of decreasing R_{dark} with growth temperature, such a pattern only appeared in AC-grown tamaracks. ECT4 tamarack R_{dark} was as low as the ECT8, again perhaps underpinned by the low foliar nitrogen concentration (as explained previously). While R_{dark25} decreased significantly with increasing growth temperature, Q_{10} did not respond to growth temperature, again indicating Type I acclimation of R_{dark} in tamarack. Other studies have shown that conifers are able to successfully acclimate respiration to

increasing growth temperature, even to a greater extent than broad-leaved species

however growth temperature and CO_2 concentrations were maintained at lower levels

than this project (Tjoelker et al. 1999a, Tjoelker et al. 1999b, reviewed in Way and Oren

2010).

Neither species showed a response of R_{dark} to elevated growth CO_2, nor effects on R_{dark25}

or Q_{10}. This suggests that foliar mitochondrial structure and density did not respond to

enriched growth CO_2, and changes in photosynthetic carbohydrate production did not

translate into altered rates of R_{dark} (Griffin *et al*. 2001, Armstrong *et al*. 2006b). Previous

studies on trees have found a similar lack of growth CO_2 effect on respiratory

acclimation (Crous et al. 2012, Ayub *et al*. 2014).

4.6 Effects of elevated temperature and CO_2 on foliar nitrogen

Both species showed a reduction in foliar nitrogen concentration with increasing growth

temperature. The acclimation of R_{dark} to high temperature likely resulted from a lower

energy requirement to sustain the fewer enzymes caused by lower leaf nitrogen (Tjoelker

et al. 1999b). Declining foliar nitrogen concentration likely contributed to the reduction

in spruce A_{net} in T4 and T8 warming treatments; in tamarack, the negative effects of low

nitrogen on A_{net} appear to have been counteracted by the acclimation of g_s, facilitating

higher rates of CO_2 diffusion into the needles.

There was no overall significant growth CO_2 effect on spruce leaf nitrogen concentration, implying that high CO_2 acclimation of A_{net} in spruce was not underpinned by reductions in foliar nitrogen and was rather likely a function of decreased g_s in EC-grown trees as well as a regulatory carbon-sink feedback. The uniquely low nitrogen concentration of the ECT4 spruces (compared to other EC temperature treatments) may have been low enough (i.e., below a required nitrogen threshold) to significantly reduce $A_{net,}$ whereas the overall lack of growth CO_2 effect on leaf nitrogen indicates that nitrogen concentration alone did not lead to acclimation of A_{net} to high CO_2. There was no effect of growth CO_2 concentration on tamarack leaf nitrogen concentration; however, like spruce, there was a significant reduction in leaf nitrogen of ECT4 tamaracks. As was the case with spruce, the low nitrogen concentration of ECT4 trees may have caused reduced tamarack A_{net} in the ECT4 treatment.

4.7 Effects of elevated temperature and CO_2 on tree growth

Black spruce seedlings showed a decreasing trend in height with increasing growth temperature. Previous work with black spruce has similarly found that high temperature-grown seedlings show impaired growth, both above- and belowground (Way and Sage 2008b). There was, however, a strong positive effect of elevated growth CO_2 in spruce height, such that ECT8 trees were as tall as ACT0 trees; this suggests that predicted rises in CO_2 by the end of the century may be sufficient to offset the detrimental effects of elevated temperature on spruce height. Tamarack shoot height increased with moderate warming, while extreme warming caused a slight decline in height. An increase in shoot height with moderate warming, coupled with the constructive adjustments seen in A_{net} of

ACT4 tamarack, suggests that tamarack seedling growth will benefit with a slight increase in global temperature. However, previous work that found reduced allocation to root mass in high temperature-grown conifers (a parameter not measured in my thesis) suggests that improvements in aboveground growth with warming may be counteracted by impaired ability to access belowground resources (Way and Sage 2008b), which could increase drought susceptibility.

With extreme warming of 8 °C, black spruce stem diameter decreased relative to the T0 and T4 treatments. Overall, spruce stem diameter benefited from enriched growth CO_2 concentrations as EC spruce seedlings had a greater stem diameter than AC trees. The positive effect of elevated growth CO_2 was not sufficient to counteract the negative effect of extreme warming on spruce stem diameter. In both CO_2 treatments, tamarack stem diameter increased with moderate warming, but decreased with extreme warming. Diminishing stem diameter under extreme warming treatments suggests less carbon allocation to wood in the seedlings of both species and is consistent with decreased rates of A_{net} in warm-grown trees. Lignin formation in wood is a major carbon sink for trees and forms up to 20 % of the carbon sink in needle-leaved species (Thompson and Randerson 1996); lignin is also a recalcitrant carbon compound which decomposes slowly in forest soils, making it an effective form of long-term carbon sequestration (De Deyn et al. 2008). Whereas tamarack showed an increase in stem diameter of T4 seedlings, spruce did not – this suggests that tamarack seedlings may have an improved capability to survive in a future, warmer boreal forest compared to black spruce. Previous

dendroclimatological work has shown that field-grown black spruce radial growth was negatively affected by increasing temperatures (Huang et al. 2010).

Black spruce LMA decreased with increasing growth temperature, with the exception of ECT4 seedlings, which had a higher LMA than ECT0 trees. This result is surprising given that A_{net} in ECT4 spruce seedlings was lower than ECT0 seedlings; one would therefore expect less allocation of carbon to needle biomass. However, this was not the case. Perhaps allocation to needles mass came at the expense of allocation elsewhere, such as root mass. There was no effect of growth CO_2 concentration on spruce LMA. Tamarack LMA also decreased with increasing growth temperature and, like spruce, did not respond to growth CO_2. Decreasing LMA suggests thinner needles in both species which would facilitate increased CO_2 diffusion into the chloroplasts in warm-grown trees (Hultine and Marshall 2000).

4.8 Feedback on future climates

Black spruce and tamarack are dominant species of the boreal forest and the results of my experiment suggest that net carbon fluxes will be reduced in both species in climates predicted for the end of the 21st century. Tamarack may experience a slight increase in growth with moderate warming; however, black spruce A_{net} acclimated detractively in all warming scenarios, and growth was suppressed in spruce, even though R_{dark} was reduced by high growth temperatures. Together this suggests that these two species will not be as effective carbon sinks in the future as they are now. Reduced photosynthetic CO_2 uptake

by two major species in the boreal forest, caused by increased temperatures, could cause

a significant accumulation of atmospheric CO_2, perpetuating further climate warming

into the 22nd century.

4.9 Future directions

The greatest limitation in the design of my experiment was the sample size of five

seedlings for all the gas exchange analyses. Ideally, this experiment could be replicated

with at least one more Li-Cor 6400 XT in order to double the sample size. Additionally,

increasing the time scope of the experiment would be useful; all the seedlings in this

experiment were less than six months old. By measuring seedling carbon flux across

seasons, over several years, ontogenetic information about acclimation capacity could be

gained. Characterizing carbon flux of other boreal species will also be imperative in

creating high-resolution climate models, therefore I propose a similar experimental

design with other dominant boreal species such as paper birch (*Betula papyrifera*) and

trembling aspen (*Populus tremuloides*).

In understanding acclimation capacity, it is imperative to characterize photosynthetic

capacity; maximum rates of Rubisco carboxylation and rates of photosynthetic electron

transport are crucial parameters to quantify across plant functional types and traits in

order to create accurate climate models. While these parameters were not part of my own

work, they formed a substantial part of this overall project. Future studies must study

these parameters with all plant types. As the species composition changes in a warming

world, understanding soil dynamics will aid in predicting which types of plant species

will succeed, and the consequences on higher trophic levels that follow.

References

Ainsworth EA, Long SP (2017) What have we learned from 15 years of free-air CO2 enrichment (FACE)? A meta-analytic review of the responses of photosynthesis, canopy properties and plant production to rising CO_2. New Phytol 165:351–371.

Ainsworth EA, Rogers A (2007) The response of photosynthesis and stomatal conductance to rising [CO_2]: mechanisms and environmental interactions. Plant, Cell Environ 30:258–270.

Amthor JS (1991) Respiration in a future, higher-CO_2 world. Plant Cell Environ 14:13–20.

Amthor JS, Koch GW, Willms JR, Layzell DB (2001) Leaf O_2 uptake in the dark is independent of coincident CO_2 partial pressure. J Exp Bot 52:2235–2238.

Apps MJ, Kurz WA, Luxmoore RJ, Nilsson LO, Sedjo RA, Schmidt R, Simpson LG, Vinson TS (1993) Boreal forests and tundra. Water Air Soil Pollut 70:39–53.

Armstrong AF, Logan DC, Atkin OK (2006a) On the developmental dependence of leaf respiration: responses to short- and long-term changes in growth temperature. Am J Bot 93:1633–1639.

Armstrong AF, Logan DC, Tobin AK, O'Toole P, Atkin OK (2006b) Heterogeneity of plant mitochondrial responses underpinning respiratory acclimation to the cold in *Arabidopsis thaliana* leaves. Plant Cell Environ 29:940–949.

Atkin OK, Edwards EJ, Loveys BR (2000) Response of root respiration to changes in temperature and its relevance to global warming. New Phytol 147:141–154.

Atkin OK, Tjoelker MG (2003) Thermal acclimation and the dynamic response of plant respiration to temperature. Trends Plant Sci 8-343-351

Ayub G, Zaragoza-Castells J, Griffin KL, Atkin OK (2014) Leaf respiration in darkness and in the light under pre-industrial, current and elevated atmospheric CO_2

concentrations. Plant Sci 226:120-130.

Bogdanski BEC (2008) Canada's boreal forest economy: economic and socio-economic issues and research opportunities (Vol. 414). Pacific Forestry Centre

Campbell C, Atkinson L, Zaragoza-Castells J, Lundmark M, Atkin OK, Hurry V (2007) Acclimation of photosynthesis and respiration is asynchronous in response to changes in temperature regardless of plant functional group. New Phytol 176:375–389.

Ciais P, Sabine C, Bala G (2014) Carbon and other biogeochemical cycles. In Climate Change 2013: The physical ccience basis. Contribution of Working Group I to the Fifth Assessment Report of the Intergovernmental Panel on Climate Change (pp. 465-570). Cambridge University Press.

Chapin FS, Kedrowski R (1983) Seasonal changes in nitrogen and phosphorus fractions and autumn retranslocation in evergreen and deciduous taiga trees. Ecology 64:376–391.

Crafts-Brandner SJ, Salvucci ME (2000) Rubisco activase constrains the photosynthetic potential of leaves at high temperature and CO_2. P Natl Acad Sci U S A 97:13430–13435.

Coleman HD, Samuels AL, Guy RD, Mansfield SD (2008) Perturbed lignification impacts tree growth in hybrid poplar -- a function of sink strength, vascular integrity, and photosynthetic assimilation. Plant Physiol 148:1229–1237.

Crous KY, Quentin AG, Lin Y, Ellsworth DS (2013) Photosynthesis of temperate *Eucalyptus globulus* trees outside their native range has limited adjustment to elevated CO2 and climate warming. Glob Chang Biol 19:3790–3807.

Crous KY, Walters MB, Ellsworth DS (2008) Elevated CO_2 concentration affects leaf photosynthesis – nitrogen relationships in *Pinus taeda* over nine years in FACE. Tree Phys 28:607–614.

Crous KY, Zaragoza-Castells JO, Ellsworth DS, Duursma RA, Loew M, Tissue DT, Atkin OK (2012) Light inhibition of leaf respiration in field-grown *Eucalyptus saligna* in whole-tree chambers under elevated atmospheric CO_2 and summer drought. Plant Cell Environ 35:966-81.

Curry JA, Schramm JL, Ebert EE (1995) Sea ice-albedo climate feedback mechanism. J Climate 8:240-247.

De Deyn GB, Cornelissen JHC, Bardgett RD (2008) Plant functional traits and soil carbon sequestration in contrasting biomes. Ecol Lett 11:516–531.

Ellsworth DS, Reich PB, Naumburg ES, Koch GW, Kubiske ME, Smith SD (2004) Photosynthesis, carboxylation and leaf nitrogen responses of 16 species to elevated pCO_2 across four free-air CO_2 enrichment experiments in forest, grassland and desert. Glob Chang Biol 10:2121–2138.

Farquhar GD, von Caemmerer S, Berry JA (1980) A biochemical model of photosynthetic CO_2 assimilation in leaves of C_3 Species. Planta 149:78–90.

Feller U, Anders I, Mae T (2008) Rubiscolytics: fate of Rubisco after its enzymatic function in a cell is terminated. J Exp Bot 59:1615–1624.

Gauthier PPG, Crous KY, Ayub G, Duan H, Weerasinghe LK, Ellsworth DS, Tjoelker MG, Evans JR, Tissue DT, Atkin OK (2014) Drought increases heat tolerance of leaf respiration in *Eucalyptus globulus* saplings grown under both ambient and elevated atmospheric $[CO_2]$ and temperature. J Exp Bot 65:6471–6485.

Givnish TJ (2002) Adaptive significance of evergreen vs. deciduous leaves: solving the triple paradox. Silva Fenn 36:703–743.

Gonzalez-Meler MA, Taneva L, Trueman RJ (2004) Plant respiration and elevated atmospheric CO_2 concentration: cellular responses and global significance. Ann Bot 94:647–656.

Gower S, Richards JH (1990) Larches: deciduous conifers in an evergreen world. BioSci

40:818–826.

Griffin KL, Anderson OR, Gastrich MD, Lewis JD, Lin G, Schuster W, Seemann JR, Tissue DT, Turnbull MH, Whitehead D (2001) Plant growth in elevated CO_2 alters mitochondrial number and chloroplast fine structure. P Natl Acad Sci USA 98:2473–2478.

Hazel JR (1995) Thermal adaptation in biological membranes: is homeoviscous adaptation the explanation? Ann Rev Phys 57:19-42

Holaday AS (2009) The differential response of photosynthesis to high temperature for a boreal and temperate *Populus* species relates to differences in Rubisco activation and Rubisco activase properties. Tree Physiol 30:32–44.

Huang J, Tardif JC, Bergeron Y, Denneler B, Berninger F, Girardin MP (2010) Radial growth response of four dominant boreal tree species to climate along a latitudinal gradient in the eastern Canadian boreal forest. Glob Chang Biol 16:711–731.

Hultine KR, Marshall JD (2000) Altitude trends in conifer leaf morphology and stable carbon isotope composition. Oecol 123:32–40.

Hüve K, Bichele I, Rasulov B, Niinemets Ü (2011) When it is too hot for photosynthesis: Heat-induced instability of photosynthesis in relation to respiratory burst, cell permeability changes and H_2O_2 formation. Plant Cell Environ 34:113–126.

IPCC (2014) Climate Change 2014: Synthesis Report. Contribution of Working Groups I, II and III to the Fifth Assessment Report of the Intergovernmental Panel on Climate Change . IPCC, Geneva, Switzerland, 151 pp.

Jordan DB, Ogren WL (1984) The CO_2/O_2 specificity of ribulose 1,5-bisphosphate carboxylase/oxygenase - dependence on ribulose bisphosphate concentration, pH and temperature. Planta 161:308–313.

Kasischke ES, Christensen NL, Stocks BJ (1995) Fire, global warming, and the carbon balance of boreal forests. Ecol Appl 5:437–451.

Klikoff LG (1966) Temperature dependence of the oxidative rates of mitochondria in *Danthonia intermedia*, *Penstemon davidsonii* and *Sitanion hystrix*. Nature 212:529-530

Ku SB, Edwards GE (1977) Oxygen inhibition of photosynthesis. Plant Physiol 59:991–999.

Kuiters AT, Denneman CAJ (1987) Water-soluble phenolic substaces in soils under several coniferous and deciduous tree species. Soil Biol Biochem 19:765–769.

Kurz WA, Apps MJ (1999) A 70-year retrospective analysis of carbon fluxes in the Canadian forest sector. Ecol Appl 9:526–547.

Law RD, Crafts-Brandner SJ, Salvucci ME (2001) Heat stress induces the synthesis of a new form of ribulose-1,5-bisphosphate carboxylase/oxygenase activase in cotton leaves. Planta 214:117–125.

Lee TD (2005) Acclimation of leaf respiration to temperature is rapid and related to specific leaf area , soluble sugars and leaf. Funct Ecol 19:640–647.

Lemoine R, La Camera S, Atanassova R, Dédaldéchamp F, Allario T, Pourtau N, Bonnemain J-L, Laloi M, Coutos-Thévenot P, Maurousset L, Faucher M, Girousse C, Lemonnier P, Parrilla J, Durand M (2013) Source-to-sink transport of sugar and regulation by environmental factors. Front Plant Sci 4:272.

Macdonald SE, Lieffers VJ (1990) Photosynthesis, water relations, and foliar nitrogen of *Picea mariana* and *Larix laricina* from drained and undrained peatlands. Can J Forest Res 20:995-1000.

Martin TA, Hinckley TM, Meinzer FC, Sprugel DG (1999) Boundary layer conductance , leaf temperature and transpiration of *Abies amabilis* branches. Tree Phys 19:435-443

Medlyn BE, Barton CVM, Broadmeadow MSJ, Ceulemans R, Angelis P De, Forstreuter M, Freeman M, Jackson SB, Kellomäki S, Laitat E, Rey A, Roberntz P, Sigurdsson BD, Strassemeyer J, Wang K, Curtis PS, Jarvis PG, Medlyn B (2001) Stomatal

conductance of forest species after long-term exposure to elevated CO_2 concentration: a synthesis. New Phyt 149:247-264

Miroslavov EA, Kravkina IM (1991) Comparative analysis of chloroplasts and mitochondria in leaf chlorenchyma from mountain plants grown at different altitudes. Ann Bot 68:195–200.

Mooney HA, Gulmon SL (1982) Constraints on leaf structure and function in reference to herbivory. Bioscience 32:198-206.

Moore BD, Cheng SH, Sims D, Seemann JR (1999) The biochemical and molecular basis for photosynthetic acclimation to elevated atmospheric CO_2. Plant Cell Environ 22:567–582.

O'Sullivan OS, Heskel MA, Reich PB, Tjoelker MG, Weerasinghe LK, Penillard A, Zhu L, Egerton JJG, Bloomfield KJ, Creek D, Bahar NHA, Griffin KL, Hurry V, Meir P, Turnbull MH, Atkin OK (2016) Thermal limits of leaf metabolism across biomes. Glob Chang Biol 23:209-223

Ogren WL (1984) Photorespiration: pathways, regulation, and modification. Ann Rev Plant Physiol 35:415-442

Van Ommen Kloeke a. EE, Douma JC, Ordoñez JC, Reich PB, Van Bodegom PM (2012) Global quantification of contrasting leaf life span strategies for deciduous and evergreen species in response to environmental conditions. Glob Ecol Biogeogr 21:224–235.

Peng C, Ma Z, Lei X, Zhu Q, Chen H, Wang W, Liu S, Li W, Fang X, Zhou X (2011) A drought-induced pervasive increase in tree mortality across Canada's boreal forests. Nat Clim Chang 1:467–471.

Radin JW, Lul Z, Percy RG, Zeiger E (1994) Genetic variability for stomatal conductance in Pima cotton and its relation to improvements of heat adaptation. P Natl Acad Sci USA 91:7217–7221.

Raison JK, Lyons JM, Thomson WW (1971) The influence of membranes on the temperature-induced changes in the kinetics of some respiratory enzymes of mitochondria. Arch Biochem Biophys 142:83–90.

Rice EL, Pancholy SK (1974) Inhibition of nitrification by climax ecosystems. III. inhibitors other than tannins. Am Journ Bot 61:1095–1103.

Robinson CH (2002) Controls on decomposition and soil nitrogen availability at high latitudes. Plant Soil. 242:65-81.

Sage RF (1994) Acclimation of photosynthesis to increasing atmospheric CO_2: The gas exchange perspective. Photosynth Res 39:351–368.

Sage RF, Kubien DS (2007) The temperature response of C_3 and C_4 photosynthesis. Plant, Cell Environ 30:1086–1106.

Sage RF, Pearcy RW (1987) The Nitrogen Use Efficiency of C_3 and C_4 Plants. Plant Physiol 84:959–963.

Sage RF, Way DA, Kubien DS (2007) Rubisco, Rubisco activase, and global climate change. J Exp Bot 59:1581–1595.

Salvucci ME, Crafts-Brandner SJ (2004) Inhibition of photosynthesis by heat stress: the activation state of Rubisco as a limiting factor in photosynthesis. Physiol Plant 120:179–186.

Scafaro AP, Xiang S, Long BM, Bahar NHA, Weerasinghe LK, Creek D, Evans JR, Reich PB, Atkin OK (2016) Strong thermal acclimation of photosynthesis in tropical and temperate wet-forest tree species: the importance of altered Rubisco content. Glob Chang Biol doi: 10.1111/gcb.13566

Seto KC, Güneralp B, Hutyra LR (2012) Global forecasts of urban expansion to 2030 and direct impacts on biodiversity and carbon pools. P Natl Acad Sci USA 109:16083-16088.

Slot M, Kitajima K (2015) General patterns of acclimation of leaf respiration to elevated temperatures across biomes and plant types. Oecol 177:885–900.

Small E (1972) Photosynthetic rates in relation to nitrogen recycling as an adaptation to nutrient deficiency in peat bog plants. Can J Botany. 50:2227-2233.

Tang Y, Wen X, Lu Q, Yang Z, Cheng Z, Lu C (2006) Heat stress induces an aggregation of the light-harvesting complex of photosystem II in spinach Plants. Plant Physiol 143:629–638.

Thompson V, Randerson T (1996) Change in net primary production and heterotrophic respiration: How much is necessary to sustain the terrestrial carbon sink? Global Biogeochem Cy 10:711–726.

Tjoelker MG, Oleksyn J, Reich PB (1999a) Acclimation of respiration to temperature and CO2 in seedlings of boreal tree species in relation to plant size and relative growth rate. Glob Chang Biol 5:679–691.

Tjoelker MG, Reich PB, Oleksyn J (1999b) Changes in leaf nitrogen and carbohydrates underlie temperature and CO_2 acclimation of dark respiration in five boreal tree species. Plant, Cell Environ 22:767–778.

Troeng E, Linder S (1982) Gas exchange in a 20-year-old stand of scots pine. Physiol Plant 54:7-14

Warren CR, Dreyer E, Adams M a. (2003) Photosynthesis-Rubisco relationships in foliage of *Pinus sylvestris* in response to nitrogen supply and the proposed role of Rubisco and amino acids as nitrogen stores. Trees 17:359–366.

Way DA, Oren R, Kroner Y (2015) The space-time continuum: the effects of elevated CO_2 and temperature on trees and the importance of scaling. Plant Cell Environ 38:991–1007.

Way DA, Sage RF (2008a) Thermal acclimation of photosynthesis in black spruce [*Picea mariana* (Mill.) B.S.P.]. Plant Cell Environ 31:1250–1262.

Way DA, Sage RF (2008b) Elevated growth temperatures reduce the carbon gain of black spruce [*Picea mariana* (Mill.) B.S.P.]. Glob Chang Biol 14:624–636

Way DA, Yamori W (2014) Thermal acclimation of photosynthesis: on the importance of adjusting our definitions and accounting for thermal acclimation of respiration. Photosynth Res 119:89–100.

Wingler A, Lea PJ, Quick WP, Leegood RC (2000) Photorespiration: metabolic pathways and their role in stress protection. Philos Trans R Soc B Biol Sci 355:1517–1529.

Yamori W, Hikosaka K, Way DA (2014) Temperature response of photosynthesis in C_3, C_4, and CAM plants: temperature acclimation and temperature adaptation. Photosynth Res 119:101–117.

Curriculum Vitae

Name: Sasha Madhavji

Post-secondary University of Western Ontario
Education and London, Ontario, Canada
Degrees: 2010-2015 B.Sc. (Hons)

      The University of Western Ontario
      London, Ontario, Canada
      2015-2017 M.Sc.

Honours and Society of Graduate Students Teaching Award Nominee
Awards: 2016 and 2017

      Department of Biology Travel Award
      2017

Related Work Teaching Assistant
Experience   The University of Western Ontario
      2015-2017

Presentations Canadian Society for Plant Biologists 2017
      Ontario Climate Symposium 2017
      Ecological Society of America 2017